

SOME PROPERTIES OF NATURALLY OCCURRING RADIATIONS AND RADIOACTIVE IONS IN THE ATMOSPHERE

MINORU KAWANO, YUKIMASA IKEBE, YOSHIYUKI NAKASHIMA,
and KUNIYASU SHIMIZU

Department of Nuclear Engineering

(Received October 31, 1965)

Abstract: This paper is consisted of two parts. Chapter 1 is concerned with the ionizations by the alpha-, beta-, and gamma-radiations from the atmosphere and the ground. The specially designed ionization chamber and the plastic wall ionization chamber are used for measuring the rate of ion pair production by the beta-, and gamma-radiations respectively. The charcoal trapping method is used for measuring the rate of ion pair production by the alpha-radiation. The survey was carried out at 32 points in and around Nagoya City. The beta-radiation plays the largest contribution for the ionization of the air near the ground, and the gamma-radiation including cosmic-ray is the next. The rate of ion pair production due to the alpha-radiation in the atmosphere is almost 1 J on the average. The contribution of the low energy radiation below 40 KeV for the ionization of the air close to the ground is almost the same with that of the alpha-radiation.

Chapter 2 is concerned with the properties of the radioactive ions. The energy-spectra of alpha-particles radiated from the radioactive ions in the three ranges of critical mobility were measured. The results showed that the radioactive ions of which critical mobilities being 4.4 cm²/sec V and 0.7 cm²/sec V carry only RaA, and those of which critical mobility being 0.2 cm²/sec V carry not only RaA but also RaB and RaC. The results of simultaneous measurements show that the radioactive ions of which critical mobility being 4.4 cm²/sec V only are free from any kind of condensation nuclei. The mean life of radioactive ion in the range described above is 23 sec on the mountain top, and is 1.3 sec on the campus inside a big city.

Introduction

In general, the phenomena due to the natural radioactivity in the atmosphere seem to be able to be divided into two parts; the one is concerned with the radiation of the alpha-, beta-, and gamma-rays from the ground surface and the air, and the other one is concerned with the airborne radioactivity.

The radiations from the radioactive substances contained in the earth's crust were studied mainly from the view point of geoscience at first. Hess and his collaborators studied these phenomena from the view point of the atmospheric ionization. Recently, the peaceful utilizations of atomic energy have been developed, and the naturally occurring radiation dose rate is considered to be important from the view points of the irradiation effects on human body and the back ground for the external radiation dose rate accompanied with irradiations from radioisotope sources and accelerators.

On the other hand, the time variations of the concentration of the radioactive substances in the atmosphere and its relations with the meteorological elements

were studied by many authors in the many places of the world. Until now, many important phenomena were clarified by them. But, the absolute values of the concentrations of radioactive substances and the size distributions of the radioactive aerosols are still remained to solve in the future. To prevent the radioactive substances from entering into human body by breathing is now important problem in the field of the radiation protection. In order to solve this problem, a precisely measuring method of the concentrations and the physical properties of the radioactive aerosols should be clarified at first. As is well known, the radioactive aerosols are composed of the radon daughter products and many kinds of aerosols altogether. Therefore, the most fundamental form of the radioactive aerosols may be RaA atom or RaA atom combined with molecular ion in the atmosphere. The size of radioactive ion may successively grow up by attachment to many kinds of aerosols. When a particle size is large, it may be easy to trap the aerosol particle with a filter or an electrostatic precipitator. In order to clarify the physical process of growing up of radioactive aerosol size, the properties of radioactive ions is the important object in this laboratory.

In this paper, the following problems are described.

(1) The distributions of the alpha-, beta-, and gamma-radiations near the ground in and around Nagoya City are separately observed, and the abnormal increase of radiation due to fall-out radioactivity is reported.

(2) The relation between the radioactive nuclides carried by radioactive ions and their critical mobilities and the mean lives of radioactive ions are discussed.

Chapter 1. The ionization by each component of radiations from the ground and atmosphere near the ground

1.1. Introduction

Although the ionization of the air near the ground have been studied by several authors¹⁻¹⁾¹⁻²⁾¹⁻³⁾¹⁻⁴⁾¹⁻⁵⁾¹⁻⁶⁾¹⁻⁷⁾, a large part of these measurements were restricted to the ionization by the gamma-radiation or total radiations near the ground. Hess and his collaborators measured the ionizations by the alpha-, beta-, and gamma-radiations separately, and discussed the local anomaly and time variations. The contribution of each component of the alpha-, beta-, and gamma-radiations from the air and the ground was clarified mainly by their works. They showed that the beta-, and gamma-radiations from the ground have considerably remarkable local anomaly mainly caused by the geological and geographical conditions of the ground. Recently, the artificial radioactivity accompanying nuclear explosion tests deposited on the ground surface, and its radiation seems to increase the ionization of the air from the ground¹⁻⁸⁾¹⁻⁹⁾¹⁻¹⁰⁾. As is well known, the dose rate by the naturally occurring radiations is very important for deciding the background values of any kind of radiations and radioactivity on the earth surface. In this chapter, the results of measurements of the ionizations by the alpha-, beta-, and gamma-radiations near the ground in and around Nagoya City are reported. The abnormal increase of the beta-radiation in grass and moss areas compared with those in soil area is discussed. In the cases of measurements of the ionization in this work, all detecting equipments are fixed at 1 meter high from the ground surface.

1.2. Instruments used for measuring the ionizations

Instruments used for the present works are as follows:

i) *Ionization by the alpha-radiation.* One of the present authors (M. K.¹⁻¹¹) used the differential method with two ionization chambers for measuring the rate of ion pair production by the alpha-radiation in the atmosphere. Although this method is very convenient to carry out the continuous measurements, it seems to be hard to obtain the absolute values of the rate of ion pair production by the alpha-radiation. In the present work, the rate of ion pair production by the alpha-radiation in the atmosphere was measured by the following method:

The activated charcoal of coconut is contained in a copper tubing held at a temprature of approximately -20°C with ethylene glycol in a cold box. The outdoor air is drawn with a suction pump through the charcoal. At the end of collection, the trap is heated inside an electric furnace at about 800°C , and argon gas is used for flushing the radon gas from the charcoal trap into an ionization chamber (1.5 litres). The arrangements of equipments used for the measurements are shown in Figs. 1.1 and 1.2. Radon gas emanated from the standard radium solution (^{226}Ra , $1 \times 10^{-6}\text{Ci}$) distributed by N.B.S. was used for calibrating the ionization current.

Although the concentration of radon in the atmosphere may be measured by means of this method, the influence of the wall of the ionization chamber on the

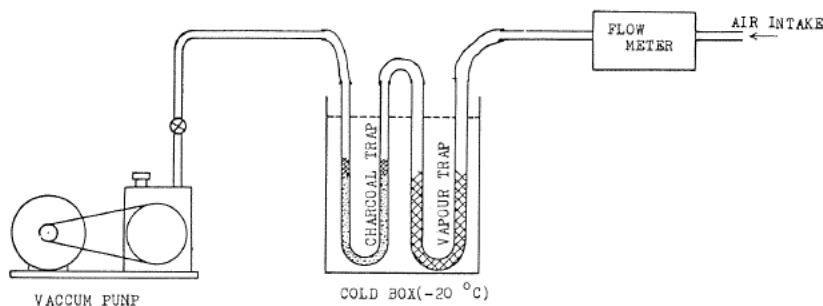


FIG. 1.1. Experimental arrangements for radon measurement. (Radon trap system.)

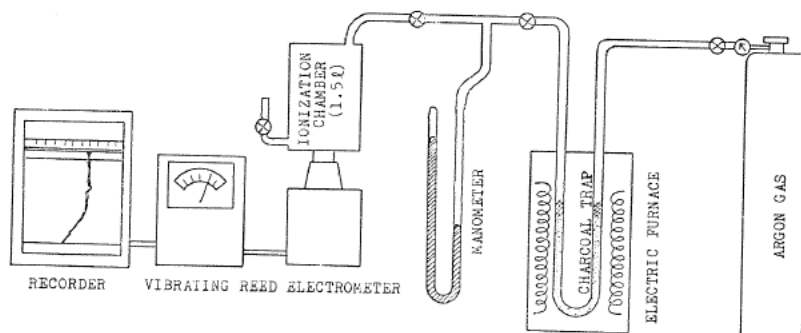


FIG. 1.2. Experimental arrangements used for radon measurement. (Measuring system used for radon concentration.)

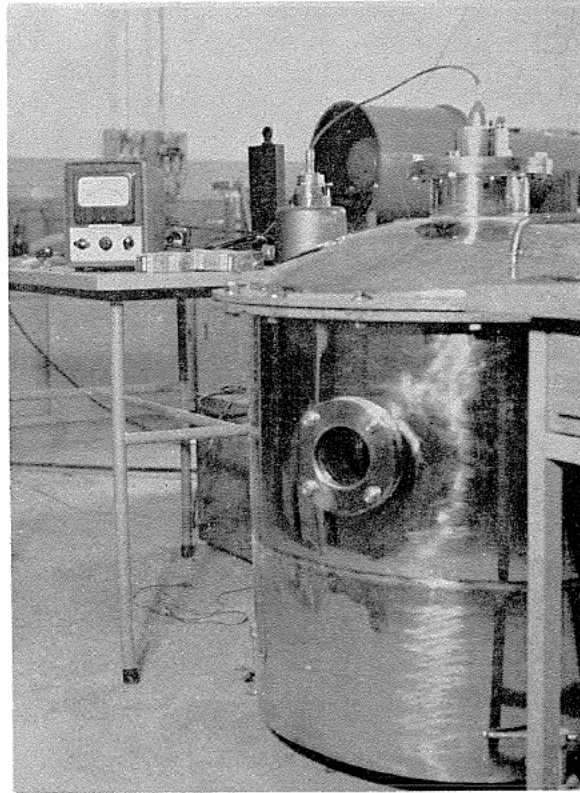


FIG. 1.3a. Large volume ionization chamber (220 litres).

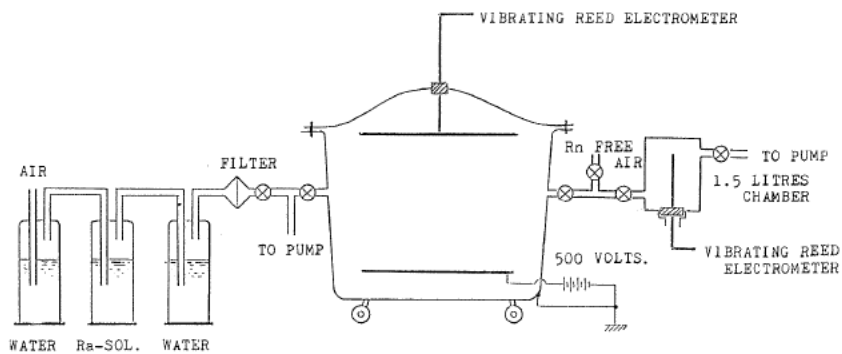


FIG. 1.3b. Arrangement used for measuring the rate of ion pair production.

ionization should be considered in the case of measuring the rate of ion pair production. In order to minimize the influence of the wall, a large volume ionization chamber is much better than that described above. Figs. 1.3a and b show the large ionization chamber and the arrangement used for measuring the rate of ion pair production. The volume of the large ionization chamber is 220 litres, but the

effective volume for ionization is 90 litres which seems to be decided by the distance between the two electrodes and the areas of the two electrodes. As the distance between the wall and the edge of electrode is 5 cm in this case, the influence of the wall on the ionization may be minimized. Both ionization chambers are initially evacuated, and the radon gas emanated from the radium solution is introduced into both ionization chambers. When the air pressure inside the chamber reaches to 1 atm pressure, the air flow through the radium solution stops. All stop-cocks for the chambers are closed. As is well known, 3 hrs. after the end of filling up is needed to keep the radioactive equilibrium inside the chamber. The rate of ion pair production may be calculated from the ionization current. Therefore, the ratio of the ionization current in the large chamber to that in the small (1.5 litres) chamber gives the ratio of the rate of ion pair production in the large chamber to that in the small chamber. The rate of ion pair production by the alpha-radiation may be obtained by multiplying the value of the rate of ion pair production measured with the small chamber by γ . The results of the measurements give 1.3 for the value of γ . The value of the ratio, 1.3, seems to be always used for obtaining the rate of ion production by the alpha-radiation in the atmosphere.

ii) Ionization by the beta-radiation. The ionization chamber used for measuring the rate of ion pair production by the beta-radiation is shown in Figs. 1.4a and b. The wall of the chamber is aluminium foil of 44 microns thick (12 mg/cm^2), and the volume is 19.2 litres (length: 61 cm, diameter: 20 cm). The alpha-particles below 9.6 MeV seem to be prevented from penetrating the wall. The collecting electrode is connected to a vibrating reed electrometer. The ionization current measured with the electrometer is recorded with an automatic recorder. The wall is kept at the potential of 180 volts which is enough for obtaining a saturation current by the beta-radiation. The ionization current measured with the chamber is due to the beta-, and gamma-radiations altogether. To obtain the current due to the beta-radiation, a stainless steel sheet is used for covering the chamber. The thickness of the sheet is 1.8 mm ($1,280 \text{ mg/cm}^2$), and is enough to absorb the beta-ray of which energy being below 2.6 MeV. Therefore, almost all beta-rays may be prevented from penetrating the steel sheet. As the gamma-

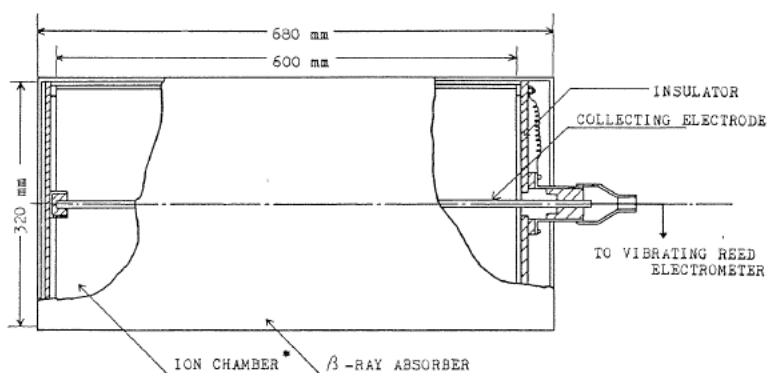


FIG. 1.4a. Ionization chamber used for measuring β -dose rate.

(* Ionization chamber was covered with aluminium foil of 12 mg/cm^2 for α -ray absorption.)

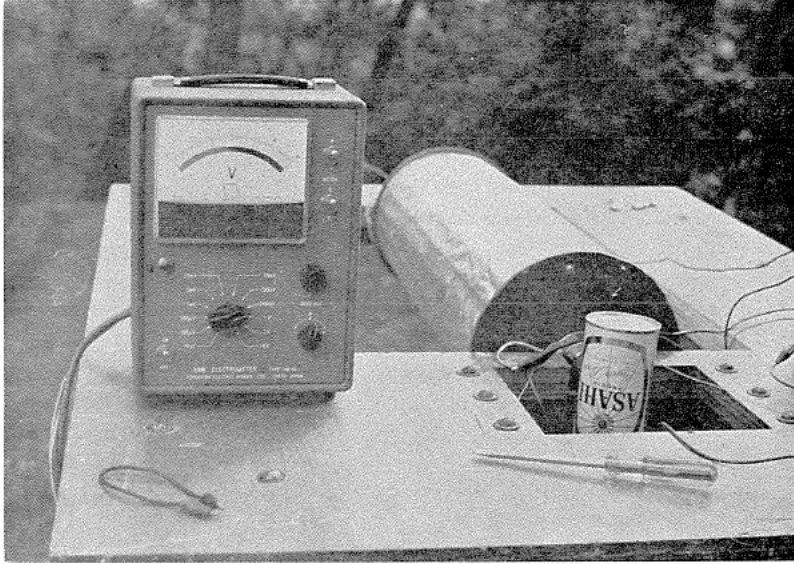


FIG. 1.4b. Photograph of ionization chamber used for the beta-radiation.
(Now, no cover is used)

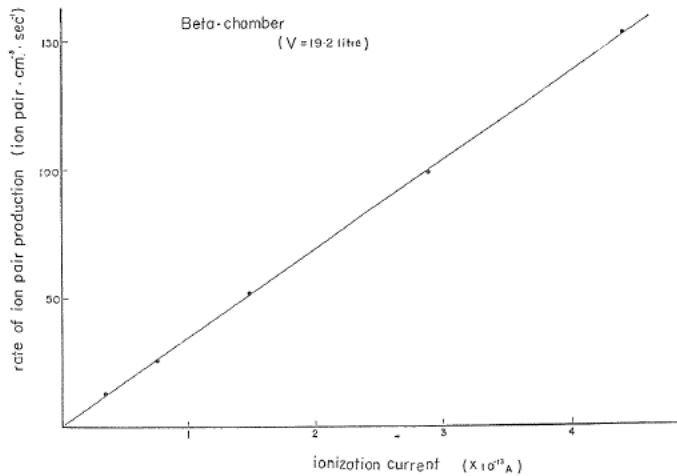


FIG. 1.5. The calibration curve of ionization current (β -chamber).

ray of which energy being above 40 KeV can penetrate the steel sheet, the difference between the ionization current measured with the chamber which is not covered by the sheet and that measured with the chamber covered with the sheet gives the ionization current by the beta-radiation only. The ionization current measured with the chamber is calibrated by the gamma-ray radiated from a standard radium (^{226}Ra) source of 5.26 mg (Fig. 1.5). As shown in the figure, the ionization current measured with the chamber is perfectly proportional to the dose rate.

iii) Ionization by the gamma-radiation. The ionization chamber used for measuring the rate of ion pair production by the gamma-radiation is shown in Figs. 1.6a and b. The wall of chamber is made by one kind of plastic plate of 5 mm thick, and the inside of wall is coated with carbon (aquadac) needed for keeping the wall to be electrostatically conductive. The volume of the chamber is 15.0 litres. The collecting electrode is an aluminium pole of which diameter being 0.5 cm. The electrode is connected to a vibrating reed electrometer. The ionization current is calibrated by the gamma-ray radiated from a standard radium (^{226}Ra) source of 5.26 mg (Fig. 1.7). The ionization current measured with the plastic chamber is due to not only the gamma-ray but also the cosmic-ray. Although it seems to be hard to measure the ionization by the residual radioactivity contained in the wall materials, the residual radioactivity contained in plastic, in general, may be very little. If some alpha-particles radiated inside the chamber, high pulses in the ionization current due to alpha-particles can be easily detected on a record, and are excluded from the data.

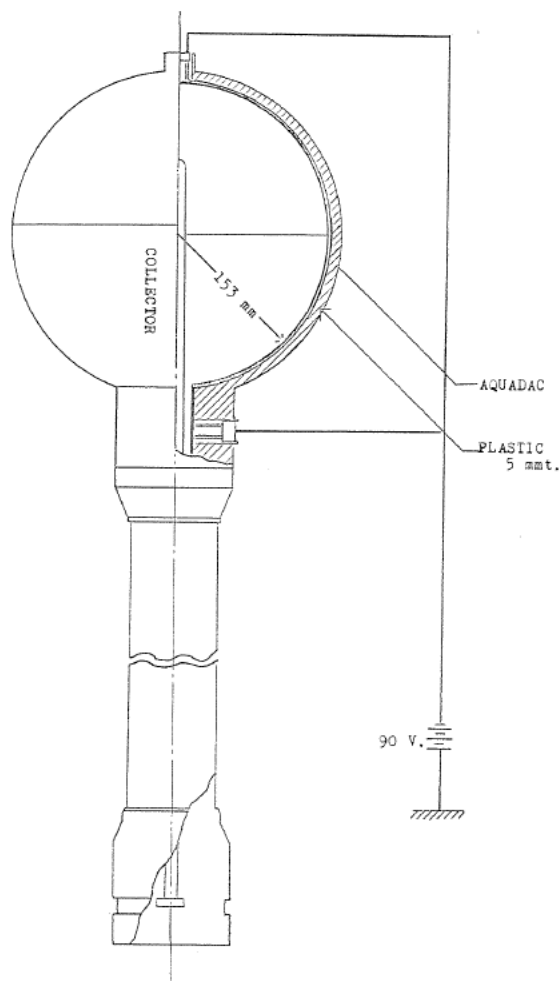


FIG. 1.6a. The ionization chamber used for measuring the gamma-radiation.

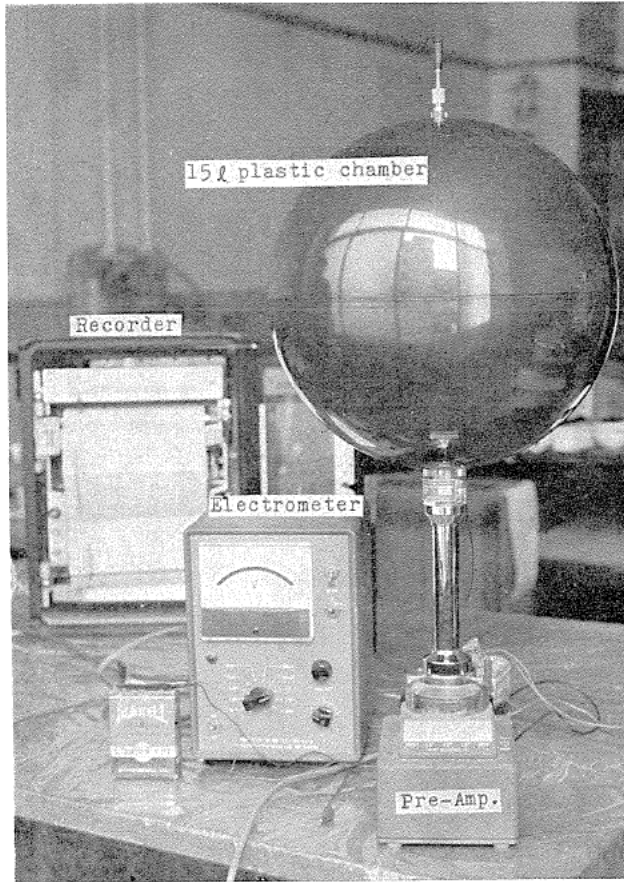


FIG. 1.6b. Photograph of the ionization chamber used for the gamma-radiation.

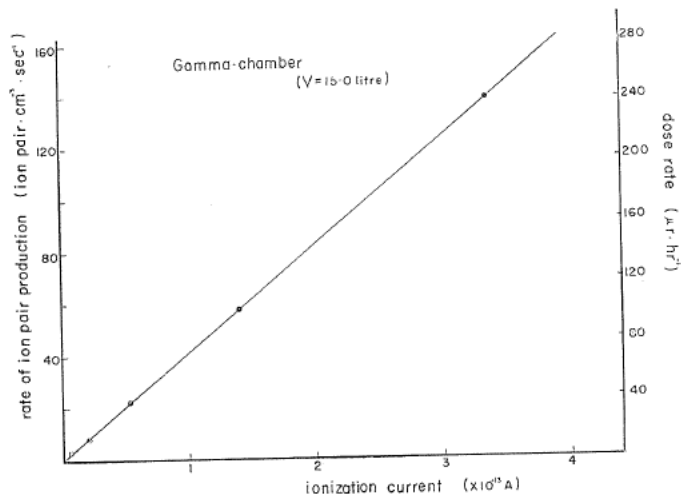


FIG. 1.7. The calibration curve of ionization current (γ -chamber).

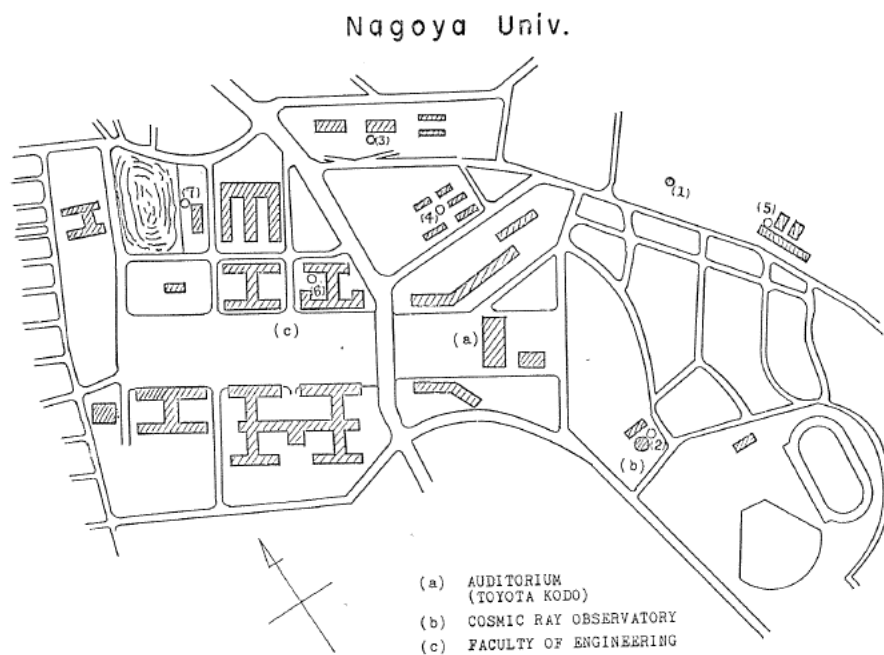


FIG. 1.8. The measuring points inside the campus.

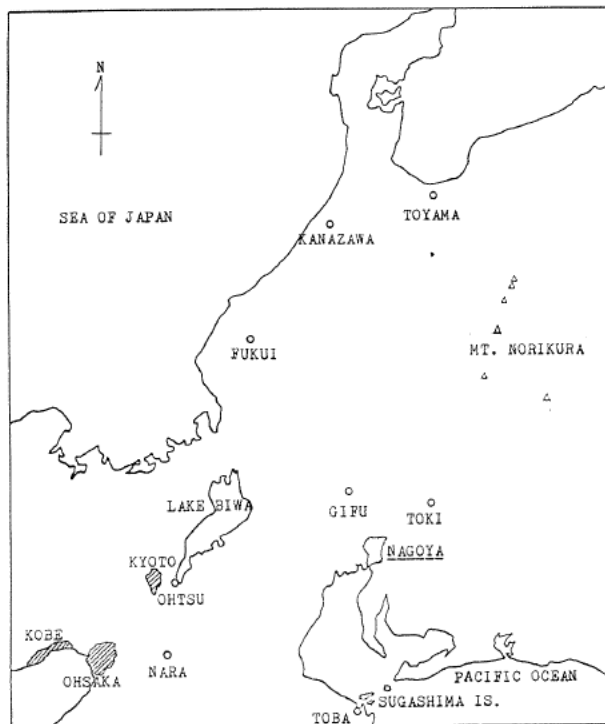


FIG. 1.9. Location of measuring points in the Central Japan.

1.3. Measurements

The measurements of the ionization by the alpha-, beta-, and gamma-radiations from the ground and the atmosphere were carried out inside and outside of the campus. Figs. 1.8 and 1.9 show the measuring points inside and outside of the campus respectively. The campus is situated on the hill about 80 meters above the sea level in the east part of Nagoya City. The turbidity originated

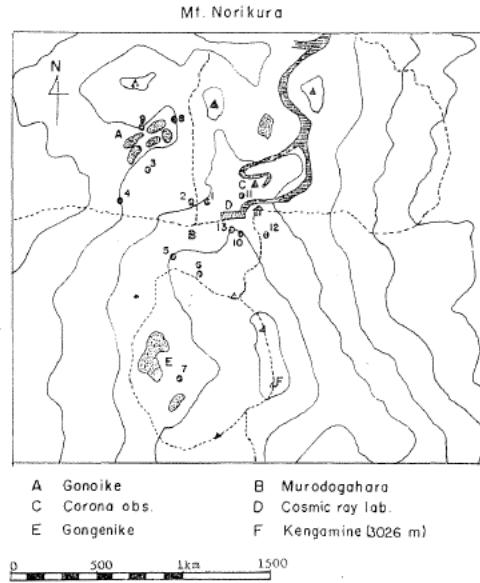


FIG. 1.10a. The measuring points on the top of Mt. Norikura.



FIG. 1.10b. The Cosmic Ray Observatory, Univ. Tokyo, Mt. Norikura.

in the central part of the city comes to this area by the wind, but is not so heavy. About one half of the ground surface inside the campus is covered by grass and trees, and the other part is just soil. The ground surface conditions of the measuring points inside the campus are shown in the Table 1.1. The measurements of the ionization by each radiation were carried out at every stations shown in Figs. 1.8, and the data were obtained on fine and very fine days. As is well known, the precipitations affect the radiations in the atmosphere. The same measurements with those inside the campus were carried out on the top of Mt. Norikura (2,770 meters high).

Fig. 1.10a shows the measuring points there. The ground surfaces of some places are covered by grass and small trees, and the surfaces in the other area are almost soil. The ground conditions are noted in Table 1. To discuss the reliability of the obtained results of measurements, the amplitude of fluctuations of the time variations should be clarified. Therefore, the continuous measurements of ionization by each radiation were carried out in the point (6) inside the campus (see Fig. 1.8).

1.4. Results

Some examples of the diurnal variation curves of the rate of ion pair production by the alpha-radiation obtained inside the campus are shown in Fig. 1.11. The maximum value appeared in the early morning, and the minimum value in the afternoon. The amplitude of this curve is not so small, and the mean value on one day is considerably different from that on the other day. The frequency distribution of the rate of ion pair production by the alpha-radiation at the point (6) is shown in Fig. 1.12. Although the maximum value is 5.9 J, the most frequent value is 0.8 J. The mean value of the rate of ion pair production by alpha-radiation is about 1.0 J.

Some examples of the diurnal variation curve of the rate of ion pair production by the beta-radiation are shown in Fig. 1.13. The amplitude of the diurnal

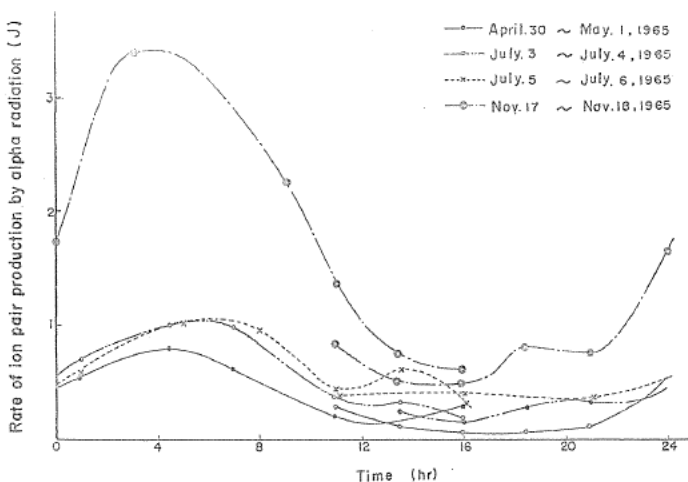


FIG. 1.11. Some examples of the diurnal variation curve of the rate of ion pair production by the alpha-radiation in the atmosphere.

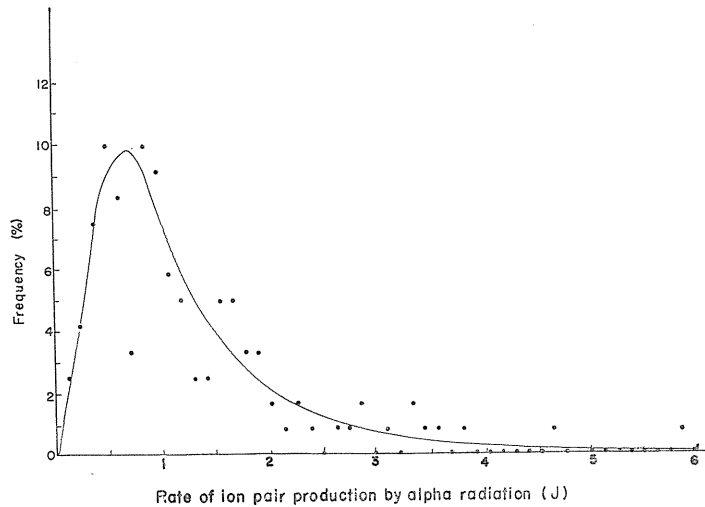


FIG. 1.12. The frequency distribution of the rate of ion pair production by the alpha-radiation in the atmosphere.

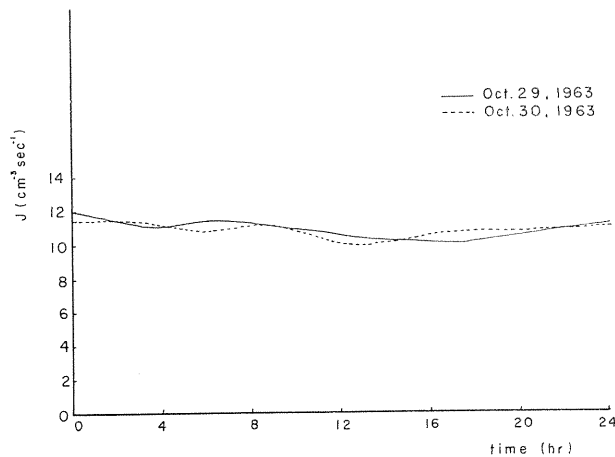


FIG. 1.13. Some examples of diurnal variation of beta-radiation.

variation curve is about 10 per cents, and the mean value is about 11 J on the soil. The maximum value appears in the early morning, and the minimum in the afternoon, and this mode of the diurnal variation curve is quite the same with that of the alpha-radiation. To explain that the amplitude of the diurnal variation curve of the rate of ion pair production by the beta-radiation is much smaller than that by the alpha-radiation, an experiment for obtaining the ratio of the ionization by "air radiation" to that by "terrestrial radiation" was carried out at the point (6). Fig. 1.14 shows arrangement of the instruments. To prevent the beta-radiation from the ground surface from penetrating the wall of the ionization chamber, the wooden plate of 30 mm thick (5 m × 5 m wide) was used

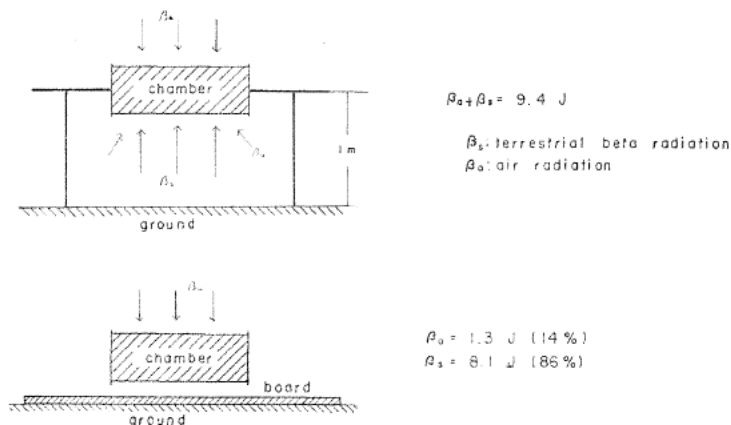


FIG. 1.14. Arrangement used for separating beta-radiation.

for covering the ground surface beneath the chamber. When the rate of ion pair production by the beta-radiation from the air and ground was 9.4 J, that by the beta-radiation only from the air was 1.3 J. Therefore, the rate of ion pair production by the beta-radiation from the ground surface is 8.1 J. The ionization by the beta-radiation from the air is almost 15 per cents, and that from the ground is about 85 per cents. As is well known, the beta-, and gamma-radiations from the ground don't change with time on fine days. Accordingly, the diurnal variation of the rate of ion pair production by the beta-radiation may be due to the radiation from the air which is only about 15 per cents of total beta-radiation. Almost all radiations may be due to the air radiation in the case of the alpha-radiation. Therefore, the amplitude of the diurnal variation of the beta-radiation should be much smaller than that of the alpha-radiation. The rate of ion pair production by the gamma-radiation doesn't change with time on fine days.

The results of measurements of the rate of ion pair production in the several points are shown in Table 1.1. As shown in this table, the contribution of the beta-ray for the ionization of the air near the ground is the most important, and the gamma-ray is the next. The contribution of the alpha-ray is not so remarkable as the beta-, and gamma-rays. The ionization by the gamma-radiation is almost the same each other in every points on the campus and the mountain top respectively. The mean value of the mountain top is almost 1.4 times larger than that on the campus. As the cosmic-ray intensity on the mountain top is much larger than that on the campus, the ionization by the cosmic-ray on the top should be much larger than that on the campus. The ionizations by the gamma-radiation in the several places in Kwanto District (around Tokyo), Nagoya, and Kwansai District (around Osaka) seem to be almost the same each other, but, the value obtained in Gifu City seems to be considerably higher than those in the other places. In the case of the beta-radiation, the local anomaly by the geological conditions seems to be not systematic, and the difference between the ionization in the soil area and that in the grass area seems to be very remarkable. The high value of beta-radiation in the grass area may be due to the fall-out radioactivity originated from the nuclear explosion tests.

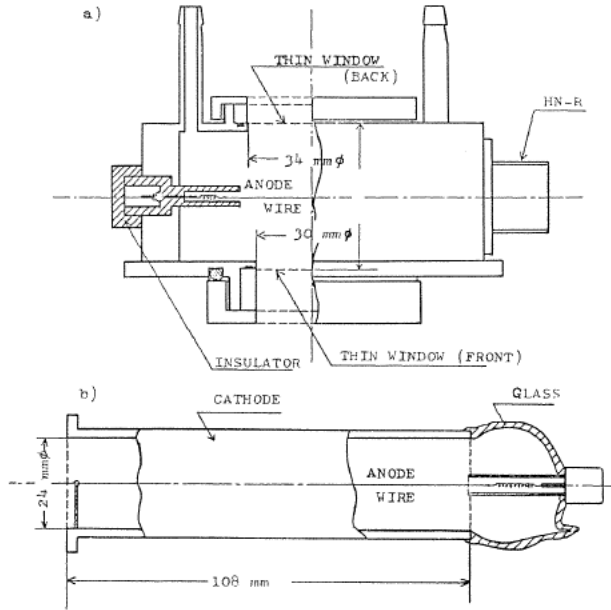
TABLE 1.1. The results of measurements of the back ground radiations in the several stations.

Stations	Surface conditions	Beta-radiation J	Gamma-radiation		
			J	$\mu\text{r/hr}$	
Nagoya Univ. Pt. 1	soil	7.0	5.1	8.8	
	2	grass	19	5.1	8.8
	3	grass	19	5.5	9.5
	4	grass	17	5.7	9.8
	5	soil	6.0	5.1	8.8
	6	soil	10	5.5	9.5
	7	soil	6.5	5.5	9.5
Mt. Norikura Pt. 1	grass	21	7.7	13.2	
	2	soil	8.6	7.8	13.4
	3	grass	16	7.7	13.2
	4	grass	22	7.8	13.4
	5	lava	9.2	7.6	13.1
	6	snow	5.3	7.2	12.4
	7	soil	9.0	7.7	13.2
	8	moss	22	7.8	13.4
	9	soil	8.7	7.5	12.9
	10	grass	20	7.7	13.2
	11	grass	13	7.7	13.2
	12	pine-needle	16	7.7	13.2
	13	grass	18	7.7	13.2
Yagoto, Nagoya Tokyo Univ. J.A.E.R.I.	grass	15	5.5	9.5	
	grass	12	5.1	8.8	
	soil	11	5.5	9.5	
	lawn	22	5.1	8.8	
	sea-shore	4.5	4.8	8.3	
Gifu City	grass	16	6.4	11	
	soil	7.0	7.3	12.5	
Toki, Gifu Pref.	out crop	—	14~92	24~160	
Kumatori, Osaka Pref.	soil	5.8	5.5	9.5	
	grass	5.8	5.5	9.5	
	lawn	8.4	6.8	12	
Sugashima Is.	lawn	7.7	4.6	7.9	

1.5. Ionization by the low energy radiation

As previously described, the beta-particle below 100 KeV and the gamma-ray below 40 KeV can not penetrate the walls of ionization chambers used for measuring the beta-radiation and the gamma-radiation respectively. The gamma-ray radiated from the radioactive substances contained in the earth crust are scattered by the soil, and the flux of the gamma-radiation below 40 KeV may be measurable in the atmosphere near the ground. Although this kind of radiation may be easily absorbed by the air, the contribution for ionization of the air near the ground may be not small. The instruments used for this measurement are as follows:

As is well known, a proportional counter is the most convenient and reliable for detecting the gamma-ray in the low energy range. In the present work, two kinds of proportional counter were used. The one is Ar-gas flow type, and is used for measuring the radiations of which energies being between 1 KeV and 10 KeV, and the other one is Xe-gas seal off type, and is used for the radiations between 5 KeV and 45 KeV. Their structures are shown in Figs. 1.15a, b and c,



c)

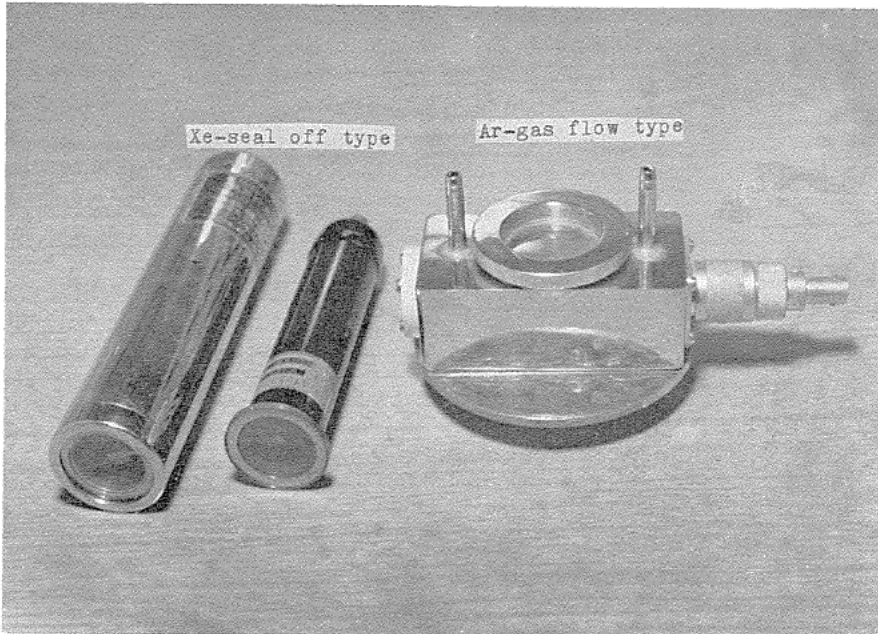


FIG. 1.15. The probes used for measuring low energy radiations.
a) Ar-gas flow counter. b) Xe-gas seal off counter. c) Photograph of these counters.

TABLE 1.2. The characteristics of the proportional counters for counting.

Proportional counter	Energy resolution	Effective length of absorber
Ar-gas flow type	20% (for MnKx)	30 (mm)
Xe-gas seal off type	10% (for BaKx)	108

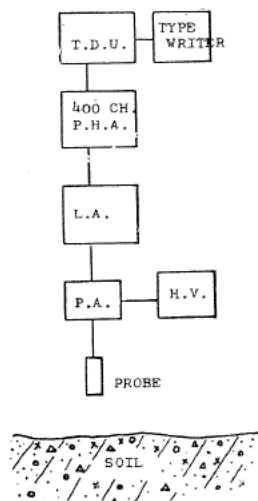


FIG. 1.16. Block-diagram of instruments used for measuring the low energy radiation.

and their characteristics for counting are shown in Table 1.2.

The energy spectra of the low energy radiations from the ground surface were measured with the proportional counters and other systems shown in Fig. 1.16. A pulse by a gamma-ray is amplified with amplifiers, and its height is analyzed with 400 ch. pulse height analyzer (Technical Measurement Corp.), and the result is automatically recorded. The windows of the proportional counters were fixed at 5 cm, 50 cm, and 100 cm above the ground surface successively. The live time of each measurement was 40 min. Some examples of the energy spectra measured with the Xe-gas seal off type counter are shown in Figs. 1.17a, b, c.

As shown in the figures, no remarkable peak in the pulse height is measured in every spectra. The countings in the energy regions above about 25 KeV seem to be a few, and the increased intensity at lower energy is due in part to the greater total absorption efficiency of the detector at lower energy and in part to the fact that the multiple scattering of the gamma-radiation occurs in the soil. Although the energy-spectrum seems to be almost the same each other, the dose rate estimated from the integrated value of each energy-spectrum is different each other; *i.e.*, the largest is the one obtained at 5 cm above the ground, the next at 50 cm, and the third at 100 cm. The rate of ion pair production by the low energy radiation measured inside the campus is shown in Table 1.3. As indicated in the table, the rate of ion pair production changes with the distance from the ground surface. It seems to be considerably important that the rate of decrement of the ionization with the distance from the ground surface is different between the soil area and the grass area. Fig. 1.18 shows the rate of ion pair production by the gamma-ray below 40 KeV near the ground surface. As indicated in Table 1.3, the ionization by the low energy radiation is not so intense as those by the radiation above 40 KeV, but, the ionization by the radiation below 40 KeV may be almost the same with that by the alpha-radiation at 1 meter above the ground. Therefore, the ionization by the radiation in the region seems to affect the electrical properties of the air close to the ground.

1.6. Conclusion

The ionization by each component of the alpha-, beta-, and gamma-radiations

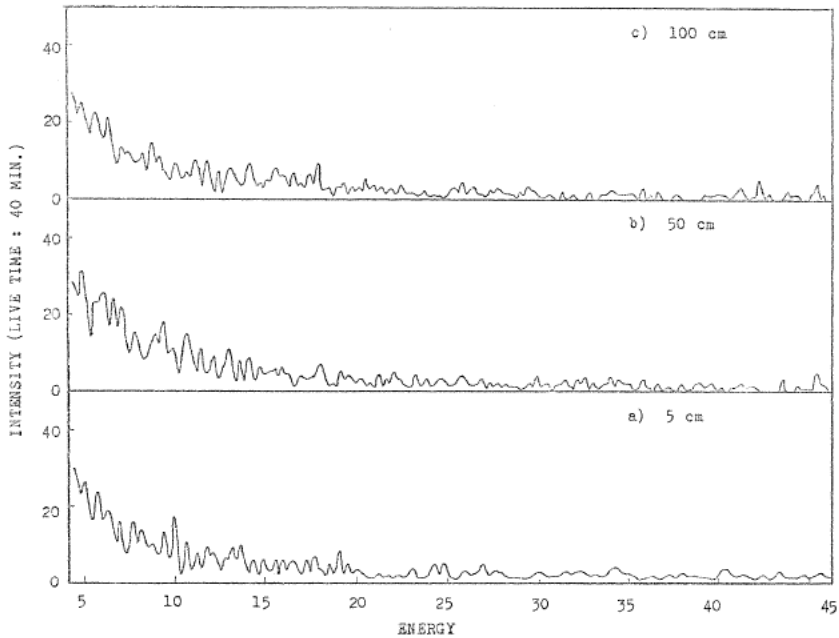


FIG. 1.17. Energy spectrum obtained with Xe-gas seal off counter. a), b), and c) are the records obtained at 5 cm, 50 cm, and 100 cm above the ground respectively.

TABLE 1.3. Ionization by the radiations below 40 KeV. (Pt. (6) inside Nagoya Univ.)

Height → Conditions ↓	5 cm (J)	50 cm (J)	100 cm (J)
moss	2.0	1.4	1.1
soil	0.8	0.7	0.6

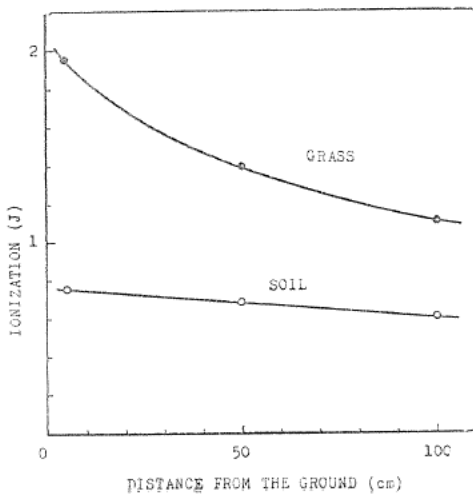


FIG. 1.18. The vertical distribution of the rate of ion pair production by the low energy radiation near the ground.

was measured separately in and around the campus of Nagoya University. The beta-radiation plays the most important role for the ionization of the air near the ground. Although the gamma-radiation including the cosmic-ray plays considerably large contribution for ionizing the air near the ground, its contribution is about one half of that of the beta-radiation even on the soil. The ionization by the alpha-radiation is small compared with those of two other radiations described above. The interesting result is obtained by the measurements of the low energy radiation near the ground. The rate of ion pair production by the radiation in this energy region is found to be almost the same with those by the alpha-radiation. The distribution of the dose rate by the low energy radiation in and around the campus will be measured in the near future.

References

- 1- 1) Hess, V. F. and G. A. O'Donnel (1951): "On the Rate of Ion Formation of Ground Level and at One Meter above the Ground". Journ. Geophys. Res., **56**, p. 557.
- 1- 2) Hess, V. F. (1953): "On the Ionization Produced by Gamma Radiation from the Ground and from the Atmosphere". Journ. Geophys. Res., **58**, p. 67.
- 1- 3) Hess, V. F., W. D. Parkinson and H. A. Miranda (1953): "Beta-ray ionization from the ground". Scientific Report No. 4, Dept. Phys. Fordham Univ.
- 1- 4) Moxham, R. M. (1964): Some Aerial Observations on the Terrestrial Component of Environmental γ Radiation. *Natural Radiation Environment.*, p. 737.
- 1- 5) Foote, R. S. (1964): Time Variation of Terrestrial γ Radiation. *Natural Radiation Environment.*, p. 757.
- 1- 6) Geyh, M. and S. Lorch (1964): Determining the Contribution of γ -rays to the Natural Environmental Radiation at Ground Level. *Natural Radiation Environment* p. 979.
- 1- 7) Watanabe, H. (1961): A New Method of Measurement of Absorption Dose Rate from Terrestrial Background Radiation. *Journal of Radiation Research* **2**, p. 61.
- 1- 8) Harris, D. L. (1955): Effects of Radioactive Debris from Nuclear Explosions on the Electrical Conductivity of the Lower Atmosphere. Journ. Geophys. Res. **60**, p. 45.
- 1- 9) Yamasaki, F. *et al.* (1964): External Doses of Radiation from Fall-out in Tokyo and its Vicinity. Journ. Rad. Res., **5**, p. 113.
- 1-10) Ishihara, T. *et al.* (1965): Measurements and Considerations of the Environmental Radiation and Radioactivities about the Site of the JAERI (1956-1963), JAERI 1079.
- 1-11) Kawano, M. and S. Nakatani (1964): Some Properties of Natural Radioactivity in the Atmosphere. *Natural Radiation Environment* p. 291.

Chapter 2. The constitution and its change of the radioactive ion

2.1. Introduction

Many authors ²⁻¹⁾ have studied the natural radioactivity in the atmosphere; in particular, the time variations of concentration of the radioactive substances, local anomaly on land and the relation between the concentration and the meteorological elements have been fairly well studied. But, the researches on the interaction between the radioactive substances and the aerosols seem to be considerably a few ^{2-2) 2-3) 2-4)}. To clarify the growing process of particle size, the original form of the radioactive aerosols and its relation with condensation nuclei should be well understood. As pointed out by Bricard and Wilkening, the radioactive ion seems to be the most fundamental form of the naturally occurring radioactive aerosols. The radioactive ions may attach to many kind of aerosols.

It is very easy to find that the daughter products of radon, RaA, RaB, and RaC, carried by the aerosols can be collected with a filter or an electrostatic precipitator. To clarify the process of attachment of radioactive ions to aerosols, the influences of condensation nuclei on the properties of radioactive ions should be studied from the view points of atmospheric physics. In this paper, the constitution of radioactive nuclides carried by the radioactive ions, the relation between the concentration of the radioactive ions and those of condensation nuclei, and the mean life of radioactive ion are discussed to study the influences of condensation nuclei on the radioactive ions.

2.2. Instruments

Although many kinds of apparatus were used for this work, the main apparatus were as follows:

(a) *Radioactive ion.* An apparatus used for collecting the radioactive ions is shown in Fig. 2.1, and is almost the same with that used by Wilkening²⁻⁴⁾. The diameter and length of the flowing tube are 25 cm and 250 cm respectively. Cu wire of 0.055 cm in diameter is supported coaxially in the flowing tube with insulators (ebonite), and is maintained at negative potentials of 90 volts, 560 volts, and 2,000 volts at need. The flowing tube is always grounded. The air is drawn through the flowing tube at the rate of 200 cm/s. For the values of potential and airflow described above, all ions collected on the wires have critical mobility larger than about $4.4 \text{ cm}^2/\text{sec V}$ (90 V), $0.7 \text{ cm}^2/\text{sec V}$ (560 V), $0.2 \text{ cm}^2/\text{sec V}$ (2,000 V). At the end of collection period, the wire is wound upon a flat spiral for activity counting. In the cases of energy-spectroscopy of alpha-particles radiated from a wire which collected the radioactive ions, a gridded ionization

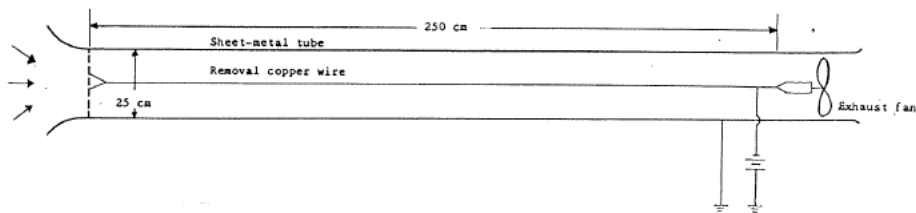


FIG. 2.1. Apparatus used for collecting radioactive ion.

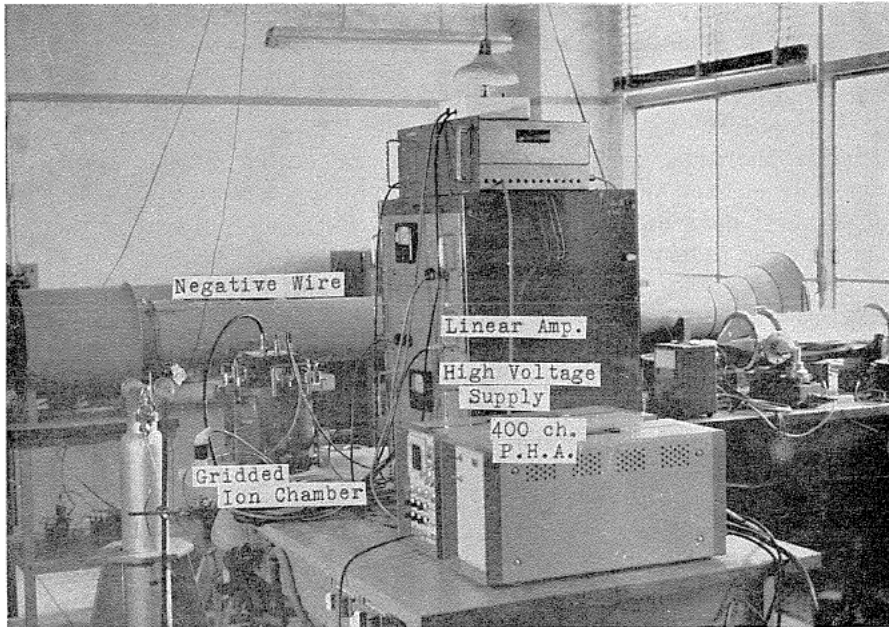


FIG. 2.2a. Experimental arrangement used for measuring alpha-energy spectrum.

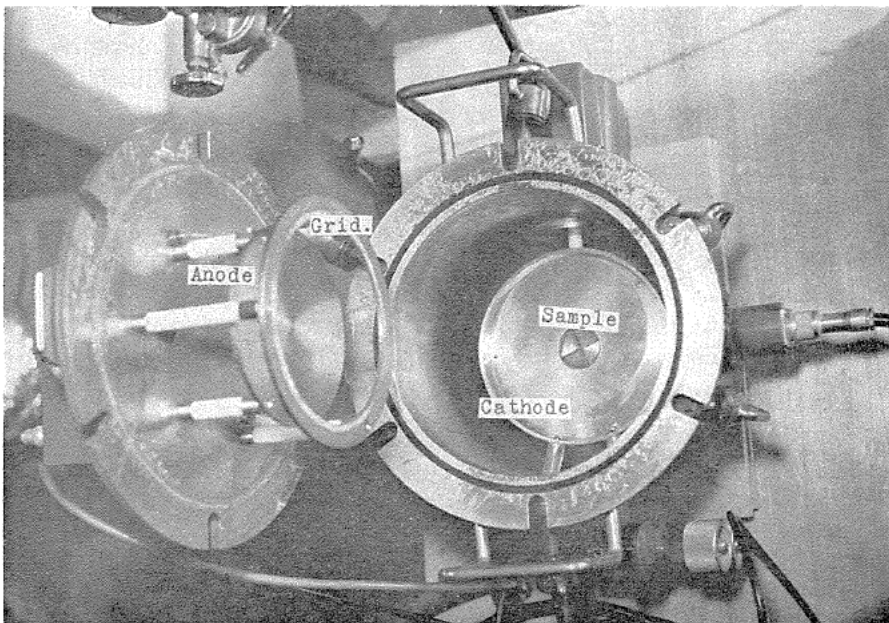


FIG. 2.2b. A view inside the gridded ionization chamber.

chamber (Osaka Dempa Co. Ltd. Japan) and a 400 ch. analyzer (Technical Measurement Corp. U.S.A.) are used for pulse height analysis. Fig. 2.2a shows the experimental arrangement used for measuring alpha-ray spectrum; *i.e.*, the radioactive ion collector, gridded ionization chamber, 400 ch. analyzer, etc. Fig. 2.2b shows the view inside the gridded ionization chamber used for the present work. PR-gas of 2 atm. is used as the counting gas. In this system, the analyzed results are automatically recorded with an electrical typewriter and cathode ray oscillograph. The accumulating time needed for obtaining a reliable counting is 40 min. for most cases because of low activity. ZnS scintillation counter is used for counting alpha-particles radiated from the wire, and the counted values are automatically recorded.

(b) *Condensation nuclei.* A Pollak aerosol counter was used for measuring the concentration of condensation nuclei. Figs. 2.3a and b show the Pollak aerosol counter used for the present work. The calibration curve obtained by Nolan²⁻⁶⁾ was used for estimating the concentration of condensation nuclei from the measured values of light absorption in the counter. Although it seems to be very hard to decide experimentally the lower limit of particle sizes of condensation nuclei which can be measured with the Pollak counter, the lower limit of particle size may be approximately estimated assuming the adiabatic expansion²⁻⁶⁾. In the case of the Pollak counter used for the present work, the lower limit of particle size may be 0.0010 microns ($=1 \times 10^{-7}$ cm).

(c) *Radon gas.* Activated charcoal kept at low temperature can trap perfectly radon gas passing through the charcoal-trap. In the present work, the activated charcoal of coconut is contained in a copper-tubing held at a temperature of approximately -20°C with ethylene glycol in a cold box. The outdoor

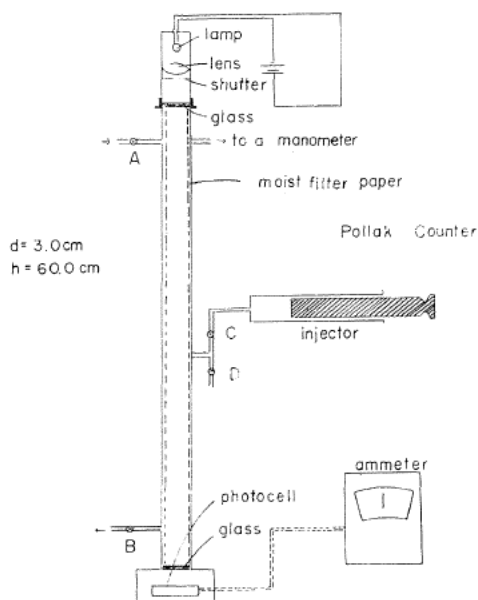


FIG. 2.3a. Schematic diagram of Pollak photo-electric aerosol counter.

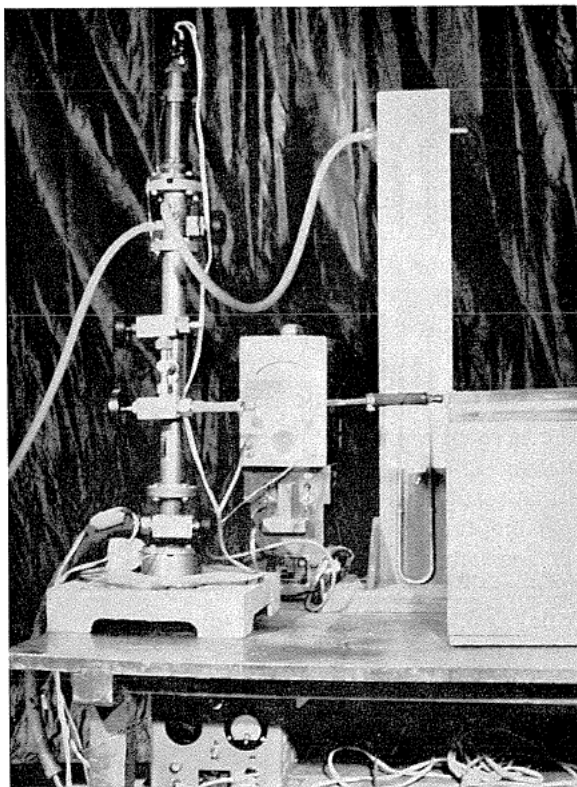


FIG. 2.3b. Pollak photo-electric aerosol counter.

air is drawn with a suction pump through the charcoal. At the end of collection, the trap is heated inside an electric furnace at about 800°C , and argon gas is used for flushing the radon gas from the charcoal-trap into an ionization chamber (1,500 cc). The ionization current due to radon is measured with a vibrating reed electrometer, and is automatically recorded. (The instruments used for measuring the radon gas are shown in Figs. 1.1, 1.2, and 1.3)

2.3. Energy spectra of alpha-particles radiated from a wire which collected the radioactive ions

A pulse height produced by an alpha-particle is directly proportional to the energy of the particle. The radioactivity of the wire was measured with a gridded ionization chamber, and each pulse height was analyzed with a 400 ch. pulse height analyzer. Figs. 2.4, 5, and 6 show the oscilloscope records of differential pulse height distribution for alpha-particles radiated from the wires maintained at the potentials of 90 volts, 560 volts, and 2000 volts respectively. Fig. 2.4a shows the three groups of alpha-particles well resolved; *i.e.*, at 6.00 MeV, 7.80 MeV, and 8.70 MeV, and these alpha-energies correspond to RaA+ThC, RaC' and ThC' respectively.

The energies of alpha-particles radiated from RaA and ThC are 5.998 MeV and 6.051 MeV respectively. It is very hard to distinguish the spectrum of 5.998

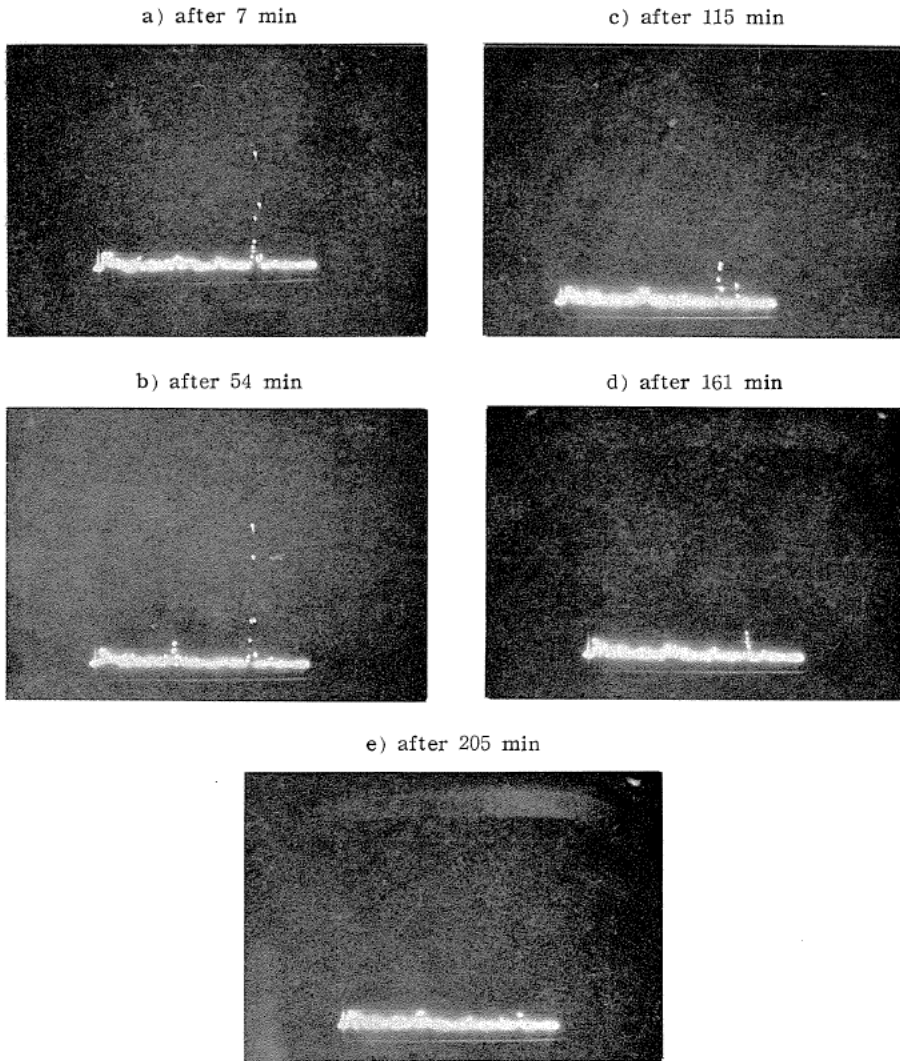


FIG. 2.4. The oscilloscope records of differential pulse-height distribution for alpha-particles radiated from the wire. (90 V)
 (Counting was accumulated during 40 min.)

MeV from that of 6.051 MeV with this kind of gridded ionization chamber. Comparing the spectrum shown in Fig. 2.4a with that in Fig. 2.4b, it is understood that the amounts of RaC' and ThC' increase rapidly, and the sum of amounts of RaA and ThC is almost constant in Figs. 2.4a and b. The spectrum of 6.00 MeV in Fig. 2.4a may correspond to RaA+ThC, and that in Fig. 2.4b may correspond to only ThC. Because, RaA decays so rapidly as it does not remain at 50 min. after the end of collection.

The oscilloscope records shown in Figs. 2.4c and d indicate the time variation of the amount of each nuclide. Although the amount of RaC' decreases

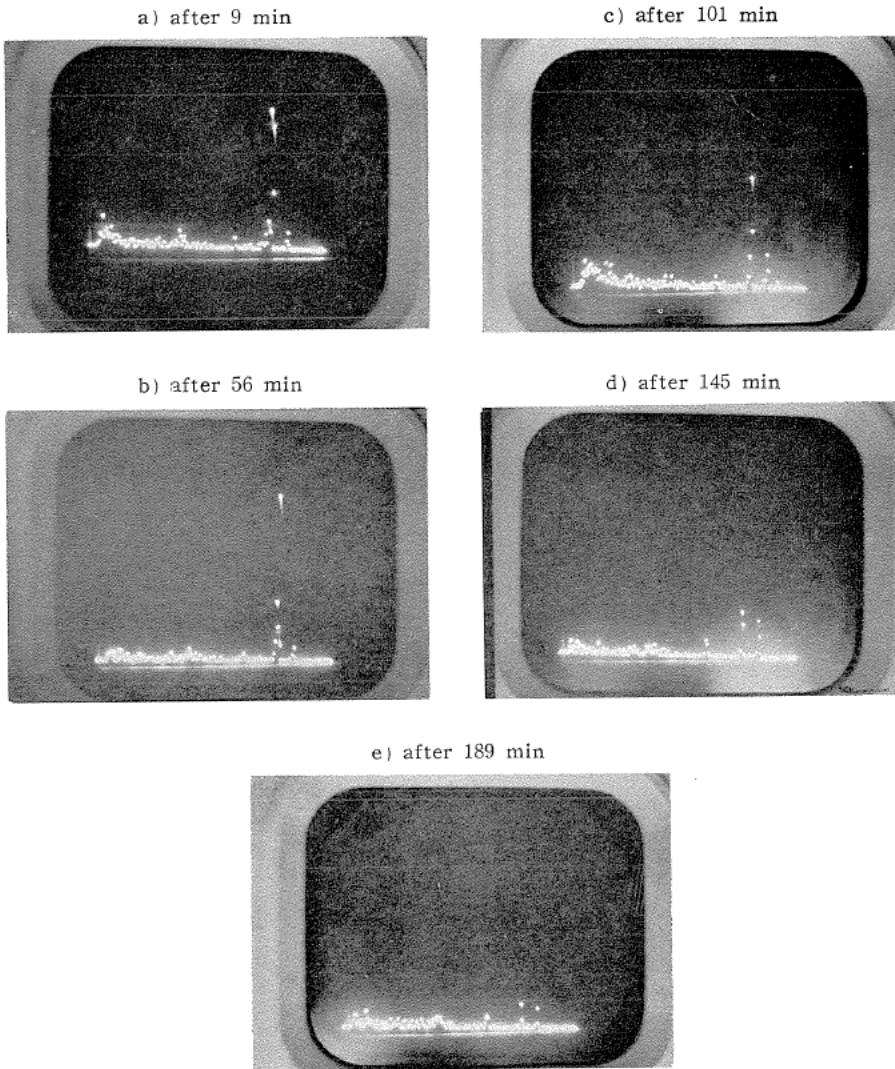


FIG. 2.5. The oscilloscope records of differential pulse-height distribution for alpha-particles radiated from the wire. (560 V)
(Counting was accumulated during 40 min)

with time, that of ThC' increases gradually, and passes through a maximum at about 100 minutes after the end of collection, and decreases gradually with time. As shown in Figs. 2.5a and 2.6a, the pulse height distribution of alpha-particles radiated from the wires maintained at the potentials of 560 volts and 2,000 volts coincide well with that from the wire maintained at the potential of 90 volts. The time variation of the radioactivity on the wire may be expressed by the following equations:

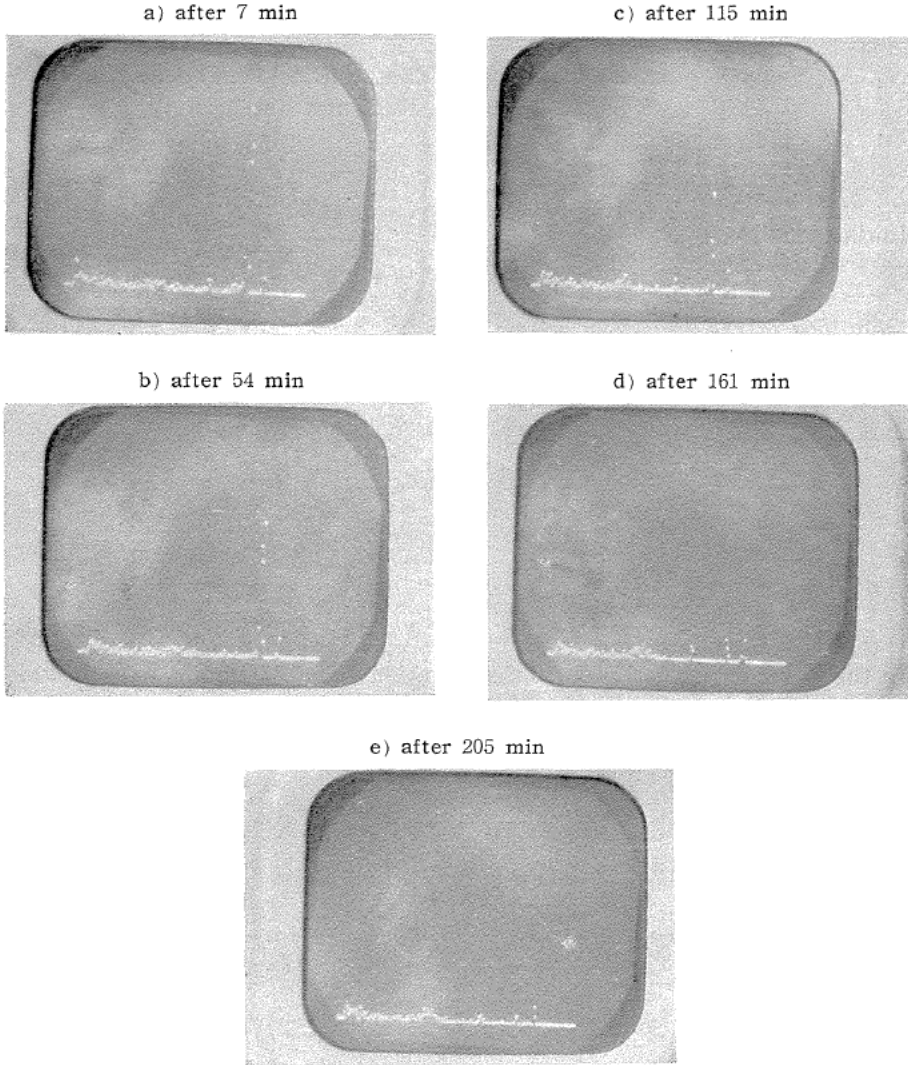


FIG. 2.6. The oscilloscope records of differential pulse-height distribution for alpha-particles radiated from the wire. (2,000 V)
(Counting was accumulated during 40 min.)

$$\frac{dN_A}{dt} = \eta q n_A - \lambda_A N_A \quad (1)$$

$$\frac{dN_B}{dt} = \eta q n_B + \lambda_A N_A - \lambda_B N_B \quad (2)$$

$$\frac{dN_C}{dt} = \eta q n_C + \lambda_B N_B - \lambda_C N_C \quad (3)$$

where,

η : collecting efficiency for radioactive ions.

q : flow rate in cc/s.

n_A , n_B , and n_C : concentrations of atoms of RaA, RaB, and RaC in the atmosphere.

N_A , N_B , and N_C : numbers of atoms of RaA, RaB, and RaC collected on a wire.

λ_A , λ_B , and λ_C : decay constants of RaA, RaB, and RaC.

λ_A : 3.79×10^{-3}

λ_B : 4.31×10^{-4}

λ_C : 5.86×10^{-4}

Initial conditions:

$$\text{at } t=0, N_A=N_B=N_C=0.$$

The solutions of the equations are as follows:

$$N_A = \frac{\eta q n_A}{\lambda_A} (1 - e^{-\lambda_A t}) \quad (4)$$

$$N_B = \frac{\eta q (n_A + n_B)}{\lambda_B} (1 - e^{-\lambda_B t}) - \frac{\eta q n_A}{\lambda_B - \lambda_A} (e^{-\lambda_A t} - e^{-\lambda_B t}) \quad (5)$$

$$N_C = \frac{\eta q (n_A + n_B + n_C)}{\lambda_C} (1 - e^{-\lambda_C t}) + \frac{\eta q \{ \lambda_C n_A + (\lambda_A - \lambda_B) n_B \}}{(\lambda_B - \lambda_A)(\lambda_C - \lambda_B)} \times \\ (e^{-\lambda_B t} - e^{-\lambda_C t}) - \frac{\eta q \lambda_B n_A}{(\lambda_B - \lambda_A)(\lambda_C - \lambda_A)} (e^{-\lambda_A t} - e^{-\lambda_C t}) \quad (6)$$

In these formulas, t expresses the duration of collection. In order to distinguish the duration of collection from the time of decay, t is exchanged with T in the formulas described above.

$$N_A^T = \frac{\eta q n_A}{\lambda_A} (1 - e^{-\lambda_A T}) \quad (4')$$

$$N_B^T = \frac{\eta q (n_A + n_B)}{\lambda_B} (1 - e^{-\lambda_B T}) - \frac{\eta q n_A}{\lambda_B - \lambda_A} (e^{-\lambda_A T} - e^{-\lambda_B T}) \quad (5')$$

$$N_C^T = \frac{\eta q (n_A + n_B + n_C)}{\lambda_C} (1 - e^{-\lambda_C T}) - \frac{\eta q \{ \lambda_C n_A + (\lambda_A - \lambda_B) n_B \}}{(\lambda_B - \lambda_A)(\lambda_C - \lambda_B)} \times \\ (e^{-\lambda_B T} - e^{-\lambda_C T}) - \frac{\eta q \lambda_B n_A}{(\lambda_B - \lambda_A)(\lambda_C - \lambda_A)} (e^{-\lambda_A T} - e^{-\lambda_C T}) \quad (6')$$

The decay of each product after the end of collection is expressed by the following equations:

$$\frac{dN_A}{dt} = -\lambda_A N_A \quad (7)$$

$$\frac{dN_B}{dt} = \lambda_A N_A - \lambda_B N_B \quad (8)$$

$$\frac{dN_C}{dt} = \lambda_B N_B - \lambda_C N_C \quad (9)$$

Initial conditions:

$$\text{at } t=0, N_A = N_A^T, N_B = N_B^T, N_C = N_C^T.$$

The solutions of these equations are as follows:

$$N_A = N_A^T e^{-\lambda_A t} \quad (10)$$

$$N_B = \frac{\lambda_A N_A^T}{\lambda_B - \lambda_A} (e^{-\lambda_A t} - e^{-\lambda_B t}) + N_B^T e^{-\lambda_B t} \quad (11)$$

$$N_C = \frac{\lambda_B \lambda_A N_A^T}{(\lambda_B - \lambda_A)(\lambda_C - \lambda_A)} (e^{-\lambda_A t} - e^{-\lambda_C t}) + \frac{\lambda_B \{(\lambda_B - \lambda_A) N_B^T - \lambda_A N_A^T\}}{(\lambda_C - \lambda_B)(\lambda_B - \lambda_A)} \times (e^{-\lambda_B t} - e^{-\lambda_C t}) + N_C^T e^{-\lambda_C t} \quad (12)$$

The alpha-counting of RaC' accumulated during $(T_2 - T_1)$ sec may be expressed as follows:

$$\begin{aligned} \int_{T_1}^{T_2} \lambda_C N_C dt = & \eta q \left[\frac{\lambda_B \lambda_C n_A (1 - e^{-\lambda_A T})}{(\lambda_B - \lambda_A)(\lambda_C - \lambda_A)} \left\{ \frac{1}{\lambda_A} (e^{-\lambda_A T_1} - e^{-\lambda_A T_2}) - \frac{1}{\lambda_C} (e^{-\lambda_C T_1} - e^{-\lambda_C T_2}) \right\} \right. \\ & + \frac{\lambda_C \{(\lambda_B - \lambda_A) n_B - \lambda_A n_A\} (1 - e^{-\lambda_B T})}{(\lambda_C - \lambda_B)(\lambda_B - \lambda_A)} \left\{ \frac{1}{\lambda_B} (e^{-\lambda_B T_1} - e^{-\lambda_B T_2}) - \frac{1}{\lambda_C} (e^{-\lambda_C T_1} - e^{-\lambda_C T_2}) \right\} \\ & + \left\{ (n_A + n_B + n_C) (1 - e^{-\lambda_C T}) + \frac{\lambda_C \{ \lambda_A n_A + (\lambda_A - \lambda_B) n_B \}}{(\lambda_B - \lambda_A)(\lambda_C - \lambda_B)} (e^{-\lambda_B T} - e^{-\lambda_C T}) \right. \\ & \left. - \frac{\lambda_C \lambda_B n_A}{(\lambda_B - \lambda_A)(\lambda_C - \lambda_A)} (e^{-\lambda_A T} - e^{-\lambda_C T}) \right\} \left. \left\{ \frac{1}{\lambda_C} (e^{-\lambda_C T_1} - e^{-\lambda_C T_2}) \right\} \right] \quad (13) \end{aligned}$$

If RaB and RaC are absent, this formula is written as follows:

$$\begin{aligned} \int_{T_1}^{T_2} \lambda_C N_C dt = & \eta q \left[\frac{\lambda_C \lambda_A n_A (1 - e^{-\lambda_A T})}{(\lambda_B - \lambda_A)(\lambda_C - \lambda_A)} \left\{ \frac{1}{\lambda_A} (e^{-\lambda_A T_1} - e^{-\lambda_A T_2}) \right. \right. \\ & \left. - \frac{1}{\lambda_C} (e^{-\lambda_C T_1} - e^{-\lambda_C T_2}) \right\} - \frac{\lambda_C \lambda_A n_A}{(\lambda_C - \lambda_B)(\lambda_B - \lambda_A)} (1 - e^{-\lambda_B T}) \\ & \times \left\{ \frac{1}{\lambda_B} (e^{-\lambda_B T_1} - e^{-\lambda_B T_2}) - \frac{1}{\lambda_C} (e^{-\lambda_C T_1} - e^{-\lambda_C T_2}) \right\} + \left\{ n_A (1 - e^{-\lambda_C T}) \right. \\ & \left. + \frac{\lambda_C \lambda_A n_A}{(\lambda_B - \lambda_A)(\lambda_C - \lambda_B)} (e^{-\lambda_B T} - e^{-\lambda_C T}) \right. \\ & \left. - \frac{\lambda_C \lambda_A n_A}{(\lambda_B - \lambda_A)(\lambda_C - \lambda_A)} (e^{-\lambda_A T} - e^{-\lambda_C T}) \right\} \left. \left\{ \frac{1}{\lambda_C} (e^{-\lambda_C T_1} - e^{-\lambda_C T_2}) \right\} \right] \\ & \equiv \eta q n_A \cdot f(T_1, T_2, T) \quad (14) \end{aligned}$$

In the case of radioactive equilibrium, there are the following relations between n_A , n_B , and n_C .

$$\begin{aligned} \lambda_A n_A &= \lambda_B n_B = \lambda_C n_C \\ n_B &= \frac{\lambda_A}{\lambda_B} n_A \quad (15a) \quad n_C = \frac{\lambda_A}{\lambda_C} n_A \quad (15b) \end{aligned}$$

Taking the relations of (15a) and (15b) into consideration, the formula (14) is written as follows:

$$\begin{aligned} \int_{T_1}^{T_2} \lambda_C N_C dt = & \eta q \cdot \left[\frac{\lambda_B \lambda_C n_A (1 - e^{-\lambda_A T})}{(\lambda_B - \lambda_A)(\lambda_C - \lambda_A)} \left\{ \frac{1}{\lambda_A} (e^{-\lambda_A T_1} - e^{-\lambda_A T_2}) \right. \right. \\ & \left. - \frac{1}{\lambda_C} (e^{-\lambda_C T_1} - e^{-\lambda_C T_2}) \right\} - \frac{\lambda_C \lambda_A n_A (1 - e^{-\lambda_B T})}{\lambda_B (\lambda_C - \lambda_B) (\lambda_B - \lambda_A)} \end{aligned}$$

$$\begin{aligned}
& \times \left\{ \frac{1}{\lambda_B} (e^{-\lambda_B T_1} - e^{-\lambda_B T_2}) - \frac{1}{\lambda_C} (e^{-\lambda_C T_1} - e^{-\lambda_C T_2}) \right\} \\
& + \left\{ \frac{\lambda_B \lambda_C + \lambda_C \lambda_A + \lambda_A \lambda_B}{\lambda_B \lambda_C} (1 - e^{-\lambda_C T}) + \frac{\lambda_C \lambda_A^2 (e^{-\lambda_B T} - e^{-\lambda_C T})}{\lambda_B (\lambda_B - \lambda_A) (\lambda_C - \lambda_B)} \right. \\
& \left. - \frac{\lambda_B \lambda_C (e^{-\lambda_A T} - e^{-\lambda_C T})}{(\lambda_B - \lambda_A) (\lambda_C - \lambda_A)} \right\} \frac{\lambda_A}{\lambda_C} (e^{-\lambda_C T_1} - e^{-\lambda_C T_2}) \Big] \equiv \eta q n_A \cdot g(T_1, T_2, T) \quad (16)
\end{aligned}$$

Theoretical curves I and II shown in Figs. 2. 7a are obtained by the numerical calculations of the formulas (14) and (16) respectively. As shown in this figure, the curve I seems to coincide well with the measured values of the amount of RaC' collected on the wire maintained at the potential of 90 volts. This good coincidence seems to support that radioactive ions collected on the wire maintained at the potential of 90 volts carry only atoms of RaA. This result coincides well with those obtained by Wilkening^{2,4)} and Bricard^{2,3,7)}. Figs. 2.7b and c show the comparisons between the theoretical curves and the measured values of RaC' collected on the wire maintained at the potentials of 560 volts and 2000 volts respectively. As shown in these figures, the theoretical curve I seems to coincide fairly well with the measured values of RaC' collected on the wire maintained at the potential of 560 volts. But, the theoretical curve I does not coincide with the measured values at the potential of 2000 volts.

These results obviously show that the radioactive ions of critical mobilities of 4.4 cm²/sec V and 0.7 cm²/sec V carry only RaA, and the ones of critical mobility of 0.2 cm²/sec V carry not only RaA but also RaB and

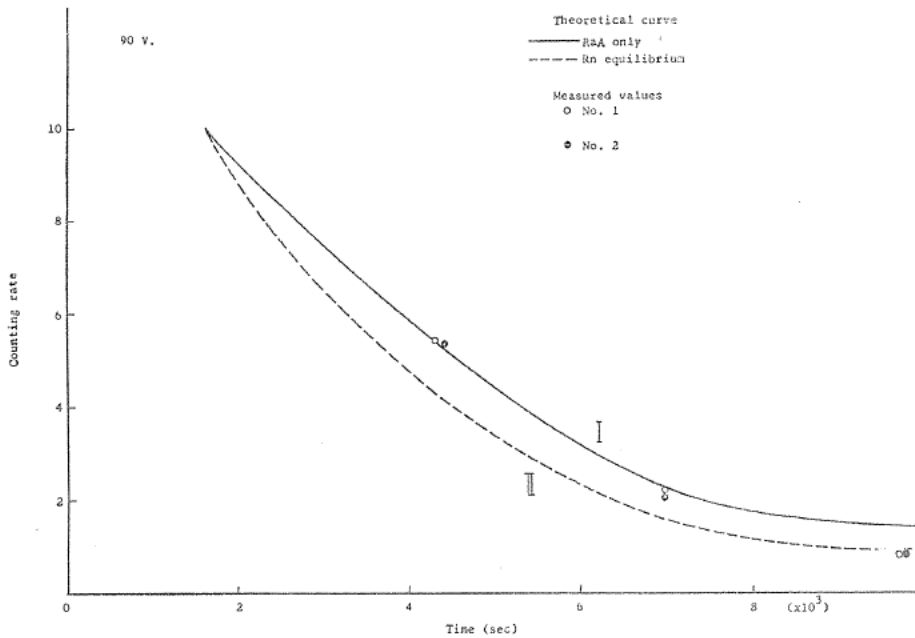


FIG. 2.7a. Decay curves of radioactivity of radioactive ions of which critical mobility being 4.4 cm²/sec V,

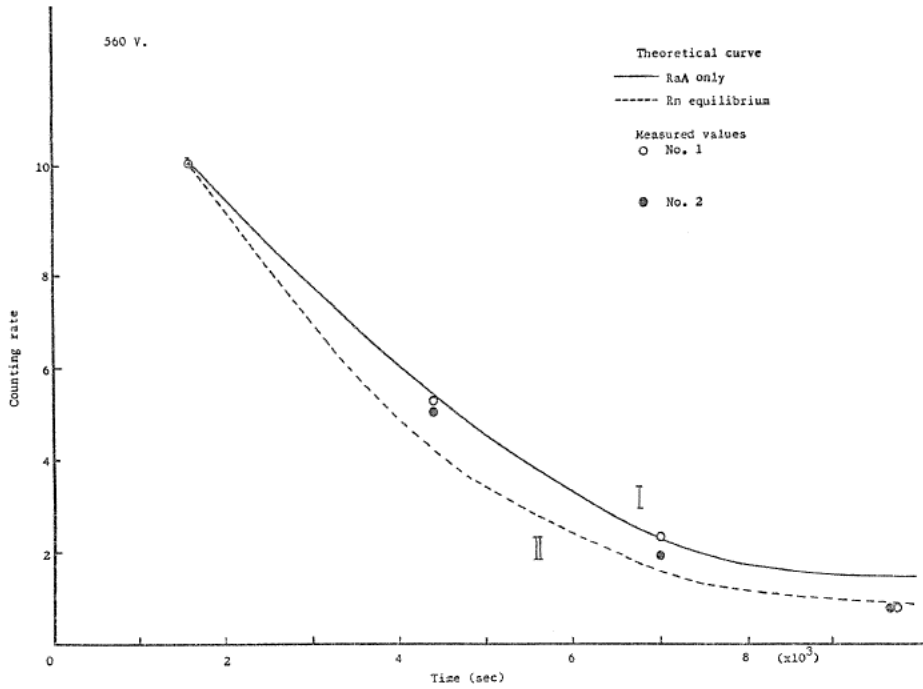


FIG. 2.7b. Decay curves of radioactivity of radioactive ions of which critical mobility being $0.7 \text{ cm}^2/\text{sec V}$.

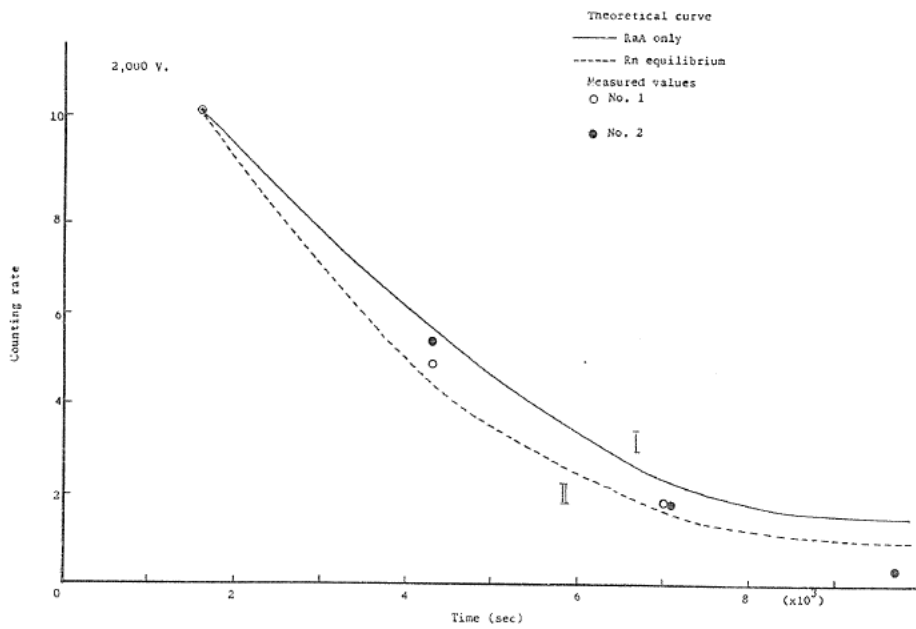


FIG. 2.7c. Decay curves of radioactivity of radioactive ions of which critical mobility being $0.2 \text{ cm}^2/\text{sec V}$.

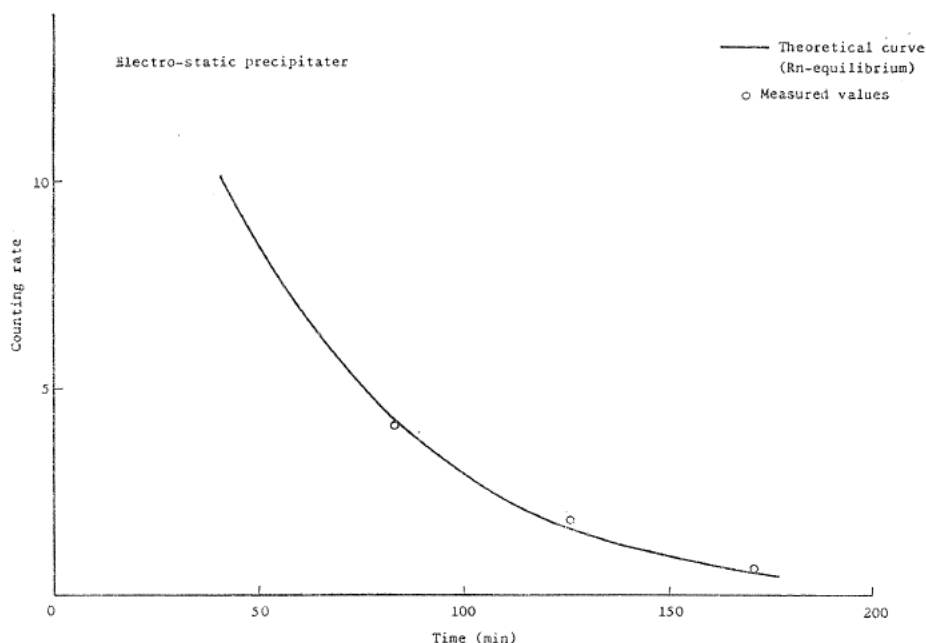


FIG. 2.7 d. Decay curves of radioactivity of radioactive aerosols collected with an electrostatic precipitator.

RaC. As previously pointed out by Kawano²⁻¹¹⁾, the radioactive nuclides carried by the radioactive aerosols collected with an electrostatic precipitator are RaA, RaB, and RaC, and there is the radioactive equilibrium between RaA, RaB, and RaC in the atmosphere. Fig. 2.7d shows the decay curves of alpha-activity collected on an electrostatic precipitator measured with the gridded ionization chamber. As shown in this figure, the theoretical curve calculated by assuming the radioactive equilibrium seems to coincide well with the measured values. Therefore, this result seems to support the conclusion described in the previous paper. As shown in Figs. 2.4, 5, and 6, the radioactive nuclides carried by the radioactive ions are not only Rn-series but also Tn-series. As the amount of ThC' on the wire is not so high as RaC', it seems to be considerably hard to discuss the radioactive equilibrium between ThA, ThB, and ThC collected on the wire.

2.4. The relation between the concentration of radioactive ions and that of condensation nuclei

The relation between the concentration of radioactive ions* and that of con-

* The concentration of the radioactive ions may be given by the following formula:

$$n_A = \frac{I_a}{0.973 \cdot q}$$

where,

n_A : the concentration of the radioactive ions in the atmosphere. (cc^{-1})

I_a : alpha-disintegration rate at the time t after the end of collection (d.p.s.) (here, t is 10 min.)

q : flow rate ($\text{cc} \cdot \text{sec}^{-1}$)

0.973 in this formula is the value at the time of 10 min. after the end of collection. The detail of this calculation is described in the previous paper (2-9),

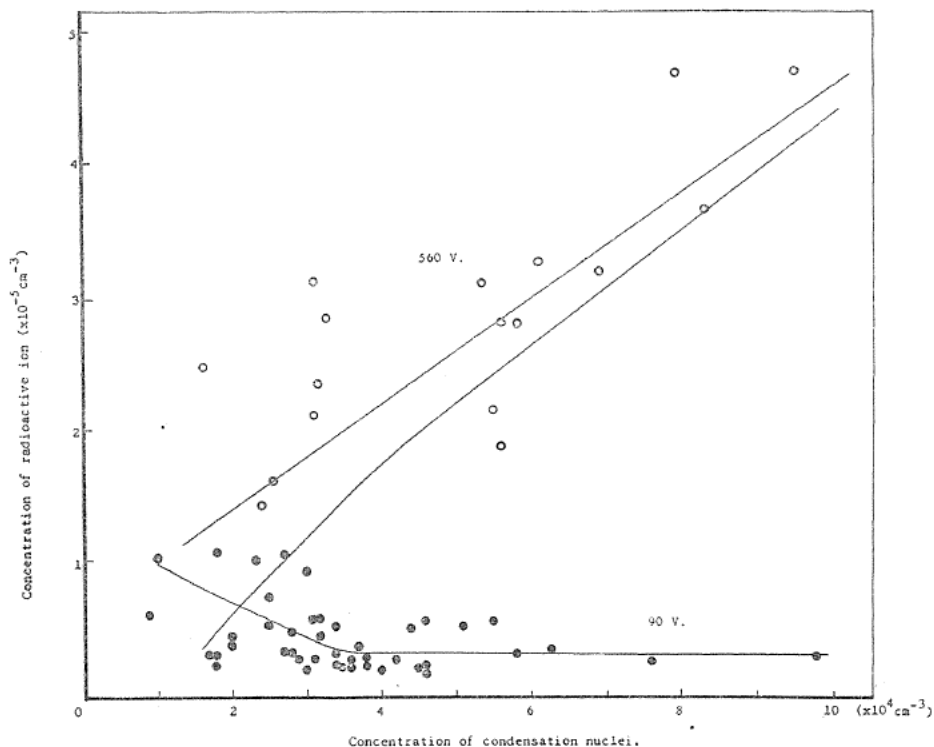


FIG. 2.8. Relation between the concentration of radioactive ion and that of condensation nuclei on the campus inside a big city.

condensation nuclei was studied on the campus of this university. As shown in Fig. 2.8, the concentration of the radioactive ions of which critical mobility being $4.4 \text{ cm}^2/\text{sec V}$ seems to be inversely proportional to that of condensation nuclei. But, the concentration of the radioactive ions of which critical mobility being $0.7 \text{ cm}^2/\text{sec V}$ seems to be almost proportional to that of nuclei.

Furthermore, the concentration of the radioactive ions of which critical mobility being $0.7 \text{ cm}^2/\text{sec V}$ is several times more than that of ions of which critical mobility being $4.4 \text{ cm}^2/\text{sec V}$ for the constant values of concentration of condensation nuclei. The results of measurements show that the concentration of radioactive ions of which critical mobility being $0.2 \text{ cm}^2/\text{sec V}$ is almost the same with that of ions of which critical mobility being $0.7 \text{ cm}^2/\text{sec V}$. The difference between the concentration of the radioactive ions of which mobility being $0.7 \text{ cm}^2/\text{sec V}$ and that of ions of which critical mobility being $4.4 \text{ cm}^2/\text{sec V}$ are shown in the same figure. To measure exactly the size distribution of radioactive ions in the range of critical mobility between $0.7 \text{ cm}^2/\text{sec V}$ and $4.4 \text{ cm}^2/\text{sec V}$ seems to be considerably hard. But, it may be recognized that the particles of which critical mobility being less than $4.4 \text{ cm}^2/\text{sec V}$ are larger than the particles of which critical mobility being larger than $4.4 \text{ cm}^2/\text{sec V}$. As described above, the concentration of radioactive ions of which critical mobility being $4.4 \text{ cm}^2/\text{sec V}$ seems to be inversely proportional to that of condensation nuclei; *i.e.*,

the radioactive ions in this range may be controlled by the process of attachment with condensation nuclei. But, the particle sizes of radioactive ions of which critical mobility being less than $4.4 \text{ cm}^2/\text{sec V}$ may be included in the range of particle size sensitive for Pollak aerosol counter. As described in this paper, the lower limit of particle sensitive for the counter may be 0.0010 microns. The remarkably different features connected with the concentration of the condensation nuclei between the radioactive ions of which critical mobility being $4.4 \text{ cm}^2/\text{sec V}$ and those of which critical mobility being $0.7 \text{ cm}^2/\text{sec V}$ seems to show the different sizes and structures between them. In the strict sense, the radioactive ions should be restricted to those which are free from any kinds of aerosols. Therefore, the radioactive ions of which critical mobility being $0.7 \text{ cm}^2/\text{sec V}$ and $0.2 \text{ cm}^2/\text{sec V}$ may be considered to be different from those of which critical mobility being $4.4 \text{ cm}^2/\text{sec V}$, and may be considered to be one kind of radioactive aerosols. Because, these ions seem to be not free from condensation nuclei.

2.5. The mean life of the radioactive ion

In the case of discussing the problems on the radioactive ion, the mean life seems to be important. To estimate the mean life of the radioactive ion, the simultaneous measurements of the concentrations of radioactive ion, radon gas, small positive ion, and condensation nuclei were carried out on the campus and the top of Mt. Norikura ($2,770 \text{ m}$ above s.l.). Mt. Norikura is one of the highest peaks in the Middle Mountain Area of Japan Island, and the Cosmic Ray Observatory and Solar Observatory of Tokyo University are situated on the top. Mt. Norikura is situated at 120 km apart from Nagoya. As the university is inside a large city—Nagoya City (population: about two millions), the atmospheric turbidity is considerably heavy. But, the air on the top of Mt. Norikura is very clean. Therefore, it seems to be very convenient to compare the several elements

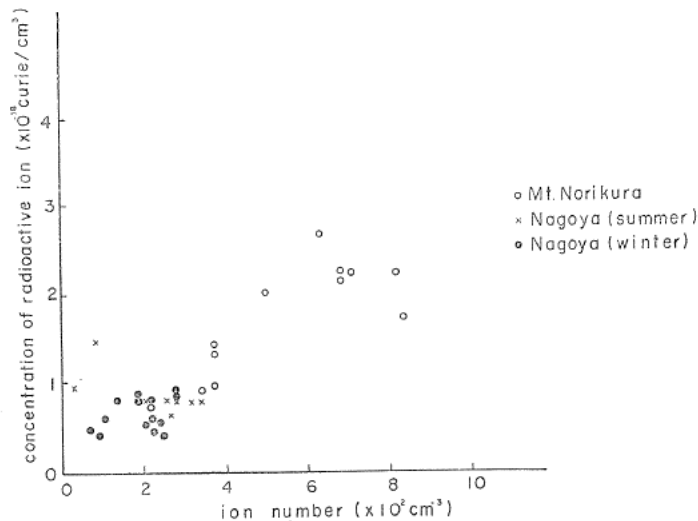


FIG. 2.9. The relation between the concentration of small positive ion and that of radioactive ion on the campus and mountain top.

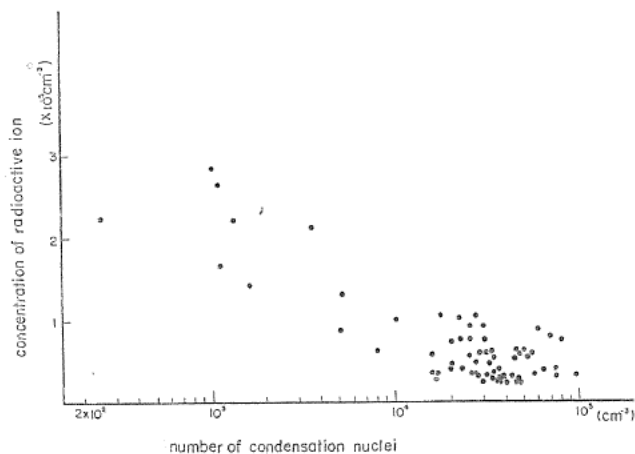


FIG. 2.10. The relation between the concentration of radioactive ions and that of condensation nuclei on the campus and mountain top.

each other in these two stations from the view point of atmospheric physics. Fig. 2.9 shows the relation between the concentration of small positive ion and that of radioactive ion obtained on the mountain top and inside the campus. The concentration of both ions are comparatively small in Nagoya owing to much turbidity. Still, the concentration of radioactive ion seems to correlate fairly well with that of small positive ion. The ratio of concentration of radioactive ion to that of small positive ion is 10^{-8} — 10^{-7} .

Fig. 2.10 shows the relation between the concentration of radioactive ions and that of condensation nuclei. The concentration of condensation nuclei on the campus is much more than that on the mountain top.

On the other hand, the concentration of radioactive ions on the campus is less than one third of that on the mountain top. The mean value of each element obtained on the mountain top and the campus is shown in the Table

The concentration of radon gas on the mountain is considerably less than that on the campus. As Mt. Norikura is considerably isolated peak, the concentration of radon gas may be less than a plain area. Assuming the radioactive equilibrium between radon and RaA, the number of atoms of RaA in the unit volume of the air may be estimated from the measured values of radon gas.

TABLE The mean values of the rate of radioactive ion production I , the concentrations of radioactive ion n , and condensation nuclei N , and the coefficient of attachment β .

	Mt. Norikura July, 1964	Nagoya University			
		Sept. 1964	Dec. 1964	May 1965	Nov. 1965
I ($\text{cc}^{-1}\cdot\text{sec}^{-1}$)	0.74×10^{-6}	4.8×10^{-6}	4.8×10^{-6}	1.5×10^{-6}	3.0×10^{-6}
n (cc^{-1})	1.7×10^{-5}	0.73×10^{-5}	0.57×10^{-5}	0.46×10^{-5}	0.45×10^{-5}
N (cc^{-1})	1.3×10^3	3.2×10^4	5.0×10^4	6.5×10^4	4.5×10^4
β ($\text{cc}\cdot\text{sec}^{-1}$)	3.4×10^{-5}	2.1×10^{-5}	1.7×10^{-5}	0.50×10^{-5}	1.5×10^{-5}

The ratio of concentration of radioactive ions which carried only RaA to that of atoms of RaA carried by every kind of aerosols (including radioactive ion) was almost 10 per cents. This value is much higher than that obtained on the campus (less than 1 per cent). The mean life of radioactive ion seems to be controlled mainly by the atmospheric turbidity which seems to be almost proportional to the concentration of condensation nuclei.

The mean life of radioactive ion may be given as follows:

$$\theta = \frac{1}{\beta N} \quad (17)$$

where,

θ : mean life of radioactive ion.

β : coefficient of attachment between a radioactive ion and condensation nucleus.

N : concentration of condensation nuclei.

Under the condition of radioactive ion equilibrium, the following relation may be given:

$$\beta = \frac{I}{nN} \quad (18)$$

where,

I : the rate of radioactive ion production. (be equal to disintegration rate of radon.)

n : concentration of radioactive ion.

Putting the value of βN shown in the Table into the formula (17), the following values of mean life of radioactive ions, θ , may be obtained.

$$\begin{array}{l} \text{Mt. Norikura :} = 23 \text{ s, campus} \\ \text{(Summer) :} = 1.4 \text{ s, (Winter) :} = 1.3 \text{ s,} \\ \text{(Spring) :} = 3.1 \text{ s, (Autumn) :} = 1.5 \text{ s.} \end{array}$$

The mean life of radioactive ion on the mountain top is much longer than that on the campus. As indicated in the Table, the values of coefficient of attachment between the radioactive ion and condensation nuclei, β , seem to be approximately constant compared with the values of other elements. Therefore, the formula (17) seems to show that the mean life of radioactive ion is inversely proportional to the concentration of condensation nuclei.

2.7. Conclusion

The energy-spectrum of alpha-particle radiated from the radioactive ions of which critical mobility being 4.4 cm²/sec V, 0.7 cm²/sec V, and 0.2 cm²/sec V were measured with the gridded ionization chamber and the 400 ch. pulse height analyzer. The results showed that the radioactive ions of which critical mobility being 4.4 cm²/sec V and 0.7 cm²/sec V carried only RaA, and the ones of 0.2 cm²/sec V carried not only RaA but also RaB and RaC. The radioactive aerosols collected with an electrostatic precipitator carried RaA, RaB, and RaC, and there was radioactive equilibrium between them. It seems to be important that the radioactive ions of which critical mobility being 4.4 cm²/sec V and 0.7 cm²/sec V carry RaA. To clarify the limit of the radioactive ions which is not held by the condensation nuclei, the relations between the concentration of the radioactive

ions in the two ranges of critical mobility and those of condensation nuclei were studied. The results of measurements on the campus show that the concentration of radioactive ions of which critical mobility being $4.4 \text{ cm}^2/\text{sec V}$ is inversely proportional to that of condensation nuclei, and the concentration of ions of $0.7 \text{ cm}^2/\text{sec V}$ is proportional to that of nuclei. Therefore, the radioactive ions of which critical mobility being $0.7 \text{ cm}^2/\text{sec V}$ seem to be held by the condensation nuclei. As the radioactive ions should be free from any kind of aerosols in the strict sense, the radioactive ions seem to be restricted to those of which critical mobility being $4.4 \text{ cm}^2/\text{sec V}$. The mean life of radioactive ion defined above was estimated from the results of simultaneous measurements of concentrations of radioactive ions, radon gas, and condensation nuclei on the campus and the mountain top. The mean life is 23 sec on the mountain top, and is 1.3–3.1 sec on the campus. It seems to be concluded that the mean life of radioactive ions is inversely proportional to the concentration of condensation nuclei. The ratio of the concentration of RaA on the radioactive ion to that of atoms of RaA is about 10 per cents on the mountain top, and is less 1 per cent on the campus. The continuous measurements of the several elements through a year were carried out on the campus inside a big city. As the concentration of the radioactive ions is low through a year, it is hard to measure the mobility spectrum of radioactive ions instead of critical mobility. But, it is important to measure the time variation of the spectrum and its relation with the concentration of condensation nuclei, and the preparations for the study are now in progress in this laboratory.

References

- 2-1) Israel, H., U. A. Krebs (1962): *Kernstrahlung in der Geophysik*, Springer-Verlag, Berlin.
- Junge, Ch., (1963): *Air Chemistry and Radioactivity*. Academy Press, N. Y.
- 2-2) Lassen, L. (1961): "The attachment of natural radioactivity to aerosols". *Geofisica pura e applicata*, **50**, p. 281.
- 2-3) Bricard, J., J. Pradel, et A. Renoux (1961): "Le Teneur de l'air en Petits et Gros Ions Radioactifs". *Geofisica pura e applicata*, **50**, p. 235.
- 2-4) Wilkening, M. H., (1964): "Radon-daughter Ions in the Atmosphere". *Natural Radiation Environment*, p. 359.
- 2-5) Nolan, P. J. and L. W. Pollak (1964): "The calibration of a photo-electric nucleus counter". *Proc. Roy. Irish Acad.*, **51**, p. 9.
- 2-6) Mason, B. J. (1957): *The Physics of Clouds* Clarendon Press, Oxford. p. 23.
- 2-7) Bricard, J. (1965): "Action of Radioactivity and of Pollution upon Parameters of Atmospheric Electricity". *Problems of Atmospheric and Space Electricity*, p. 82.
- 2-8) Kawano, M. and S. Nakatani (1964): "Some Properties of Natural Radioactivity in the Atmosphere". *Natural Radiation Environment*, p. 291.
- 2-9) Kawano, M., Y. Ikebe, and K. Shimizu: "Some Studies on the Radioactive Ions". *Journ. Meteor. Soc.* (in press).